28 Apr 1981, 2:00 pm - 5:00 pm

Analysis of Rigid Retaining Walls During Earthquakes

Shamsher Prakash
Missouri University of Science and Technology, prakash@mst.edu

Proceedings: First International Conference on Recent Advances in Geotechnical Earthquake Engineering and Soil Dynamics, April 26 - May 3, 1981, St. Louis, Missouri

Analysis of Rigid Retaining Walls During Earthquakes

Shamsher Prakash Professor in Civil Engineering,
University of Missouri-Rolla, on leave from University of Roorkee, Roorkee, India

SYNOPSIS Retaining walls experience changed pressures and undergo displacements as well during earthquakes. Both the questions have been discussed in detail in this paper. Increments in active earth pressures have been correlated with peak ground velocity and a method to compute seismic coefficient to be used in the Mononabe method has been proposed. The question of point of application of the dynamic increment has also been examined in detail. There are three methods to compute displacements of rigid retaining walls, a) based on Newmark's approach of a sliding block, b) computation of translation only and c) computation of displacements due only to rotation of the wall. All three methods have been reviewed and their limitations brought out. The questions of dynamic passive pressures, pressures on basement walls, and effect of saturation and submergence of fills need more studies. Also, there is a need to monitor behavior of walls during earthquakes and organize possibly full scale tests on test walls.

INTRODUCTION

Several types of structures are used to retain soil, e.g., cantilever sheet pilings, anchored bulkheads, flexible, and rigid (masonry) walls, Figure 1. The stability analysis of these structures necessitates the determination of earth pressures. The classical analysis of earth pressures in idealized frictional materials was initially proposed by Coulomb in 1773 for general boundary conditions. Later, Rankine (1857) analyzed them for simplified boundary conditions. Their analyses have been adopted for the purpose of determining the stability of retaining walls.

The amount of earth pressure on a retaining structure is a function of the interaction between the backfill and the structure, i.e., the deformation condition. The earth pressure on the structure, in turn, depends upon the deformation condition. Thus two factors need to be examined in a static earth pressure problem: the boundary conditions and the deformation conditions or interaction effects.

These questions have been examined at three conferences: the Brussels Conference on Earth Pressures (1958), the American Society of Civil Engineers' Specialty Conference on Lateral Stresses in the Ground and Design of Earth Retaining Structures (Cornell University, Ithaca, New York, 1970), and the Fifth European Conference on Soil Engineering (Madrid, Spain, 1970). The question of lateral pressures was also discussed in one of the specialty sessions at the Pasadena Conference in 1978. Various questions associated with magnitude and point of application of dynamic pressures, displacements of walls during earthquakes and pressures on basement walls and buried structures have been highlighted. A chronological listing of all the pertinent literature on earth pressure problems was published by Prakash et al., in 1979.

There are three categories of analytical solutions based upon the following approaches:

1. Fully plastic (static or pseudostatic) solutions
2. Solutions based on elastic wave theory, and
3. Solutions based on elasto-plastic and non-linear theory.

Nazarian and Hadjian(1979) have reviewed pertinent literature and have shown that widely different loads are obtained based on different recommendations on a typical retaining wall.

In all of the discussions on the subject, it has been recognized that there are three questions, which need to be answered in detail:

1. What is the magnitude of total (static plus dynamic) earth pressure on the structure?
2. How is the earth pressure distributed or where is the location of the center of pressure?
3. How much has the structure been displaced?

From the answers to these questions, the conditions for stability of a wall can be formulated. If the structure is located in an active seismic zone, its response to ground motion would need to be evaluated, and its stability checked during and after the seismic disturbance.

In this paper, the question of the stability of a rigid retaining wall during an earthquake is examined in detail. The effect of cohesion on earth pressure is considered in simple cases. Both pseudostatic and dynamic analyses for earth pressures and displacements available to date are reviewed. Areas, which require research in the future, are also identified.

CRITERIA FOR SATISFACTORY ACTION OF A RIGID RETAINING WALL

Before the analysis of a rigid retaining wall is undertaken, it is advisable to define the safety criteria for such a wall.

1. Stability against earth pressures.
   A wall must be safe against sliding, overturning, and bearing capacity failure caused by earth pressures acting upon it before, during and after an earthquake.
2. Estimation of displacement.
   A wall, which is safe against earth pressures, may undergo large displacement.

Thus, for earthquake conditions, one should be able to estimate the change in earth pressures from a static condition and to compute the amount of displacement during an earthquake.

DYNAMIC EARTH PRESSURES ON RIGID RETAINING WALLS

Active Earth Pressures

A retaining wall is depicted in Figure 2a. The ground motion is shown in Figure 2b. The response of this wall is sketched in Figure 2c. Consider that this retaining wall has undergone enough displacement under static conditions so that the earth pressure on it is an active earth pressure, P_A, that acts at a height of H/3 above the base. A failure wedge, abc, has also developed (Prakash, 1981).

Let the ground motion be represented by oa during the time t_1 from left to right (Fig. 2b). Because of inertia, the wall tends to move from right to left during the time interval, t_1. Let the wall movement be o_1a_1 towards the left from its original position, i.e., away from the backfill. The failure wedge, abc, also moves in the direction of the wall during the time interval, t_1.

Now, three situations can develop:

a. The rate of movement of the wall and the failure wedge can be the same. In this case, there would be no further interaction between the wall and the failure wedge. Therefore, the pressures on the wall would be unaltered at their static values.
b. The wall can move out at a rate that is higher than the rate of movement of the failure wedge. In this case, the interaction between the wall and the failure wedge would be reduced, and the earth pressure might decrease as compared to the active value under static conditions.
c. The rate of movement of the failure wedge can be greater than that of the wall. In this case, the earth pressure of the wall would increase. As a limiting condition, if it is assumed that the retaining wall does not move at all, then the increase in pressure would be at a maximum, although this is an unrealistic condition, which would not be realized in practice for free standing walls.

The interaction of the failure wedge and the backfill with the wall is a dynamic phenomenon, but the pressures are determined from pseudostatic methods.

Mononobe and Matsuo (1929) provided the first solution for the change in pressure occasioned by earthquake action by considering the inertia force that acts on the failure wedge and determining a new "total" (static and dynamic increment) earth pressure (Fig. 3). In Figure 3, a retaining wall of height, H, and inclined vertically at an angle, α, retains soil with a unit weight, γ, and an angle of shearing resistance, ϕ. The angle of wall friction is δ. The inertial force may act on the assumed failure wedge, abc_1, both horizontally and vertically where bc_1 is the trial failure surface. If a_h is the horizontal acceleration and a_v the vertical acceleration of the wedge of soil, the corresponding inertial forces are W_1a_h/g horizontally and W_1a_v/g vertically. The term W_1 indicates the weight of the wedge, abc_1. During the worst conditions for wall stability, W_1a_h/g acts toward the wall, and W_1a_v/g may act vertically, either downward or upward, during an actual earthquake. Therefore, the direction that gives the maximum increase in earth pressure is adopted in practice. Let

$$a_h/g = \alpha_h, \tag{1}$$

and

$$a_v/g = \alpha_v \tag{2}$$

in which α_h is the horizontal seismic coefficient, and α_v the vertical seismic coefficient.

The inertial forces now become $W_1\alpha_h$ and $W_1\alpha_v$ in the horizontal and vertical directions respectively. The forces acting on the wedge, abc_1, are

a. W_1, weight of the wedge abc_1 acting at its CG.
b. Earth pressure, P_1, inclined at an angle, δ, to normal, anticlockwise to the wall.
c. Soil reaction, R_1, inclined at an angle, ϕ, to normal on the face, bc_1.
d. Horizontal inertial force, $(W_1 \cdot \alpha h)$, acting at the center of gravity of the wedge, abc_1.
e. Vertical inertia force, $\pm (W_1\alpha_v)$.

Weight W_1 and the inertial forces $W_1(\pm \alpha_v)$ and $(W_1 \cdot \alpha h)$ can be combined to give a resultant, $\bar{W}_1$, such that

$$\bar{W}_1 = W_1 \sqrt{(1 \pm \alpha_v)^2 + \alpha_h^2}. \tag{3}$$

The resultant $\bar{W}_1$ is vertically inclined at an angle ψ, such that

$$\psi = \tan^{-1} \frac{\alpha_h}{1 \pm \alpha_v}. \tag{4}$$

The triangle of forces is shown in Figure 3b, and the value of P_{total} is determined; $P_{total} = P_{static} + \Delta P_{dyn}$.

The maximum value of P is then determined by considering several trial failure surfaces. This total earth pressure is made up of two components:

a. P_A - Coulomb's active earth pressure, for static condition.
b. Increase in earth pressure (ΔP_{dyn}) occasioned by an earthquake.

The point of application of P_A is H/3 above the base of the wall, whereas that of ΔP_{dyn} is recommended at 2H/3 above the base of the wall (Jacobsen, 1951) and at H/2 above the base of the wall (I.S. 1893-1975). These differences are discussed in detail later.

Coulomb's analytical expression for "total" (static + dynamic) earth pressure is as follows:

$$P_{total} = 1/2\ \gamma\ H^2\ \frac{\cos^2(\phi-\psi-\alpha)(1\pm\alpha_v)}{\cos\psi\ \cos^2\alpha\ \cos[\delta+\alpha+\psi]}\ x$$

$$\frac{1}{1+\left[\frac{\sin(\phi+\delta)\sin(\phi-i-\psi)}{\cos(\alpha-i)\cos(\delta+\alpha+\psi)}\right]^{1/2}}^{2} \qquad (5)$$

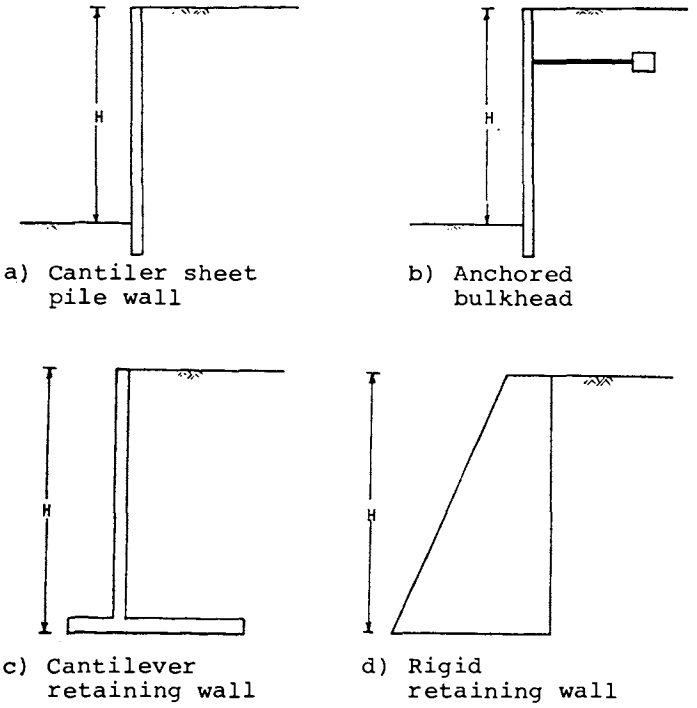

a) Cantiler sheet pile wall
b) Anchored bulkhead
c) Cantilever retaining wall
d) Rigid retaining wall

Figure 1. Different Types of Retaining Structures

A graphic method (modified Culmann's method) was developed by Kapila (1962) and has been described in detail by Prakash (1981).

Several model studies have been performed to check the validity of this analysis, and the earth pressures measured on walls subjected to sinusoidal excitation have been found to be in agreement with the computed values. In both the model tests and in a computation, the value of the acceleration is the one to which the wall is subjected. In actual ground motion, the motion is not sinusoidal. So, the question remains as to what value of seismic coefficient needs be selected for computation of total active earth pressure. Table 1 lists all pertinent analytical

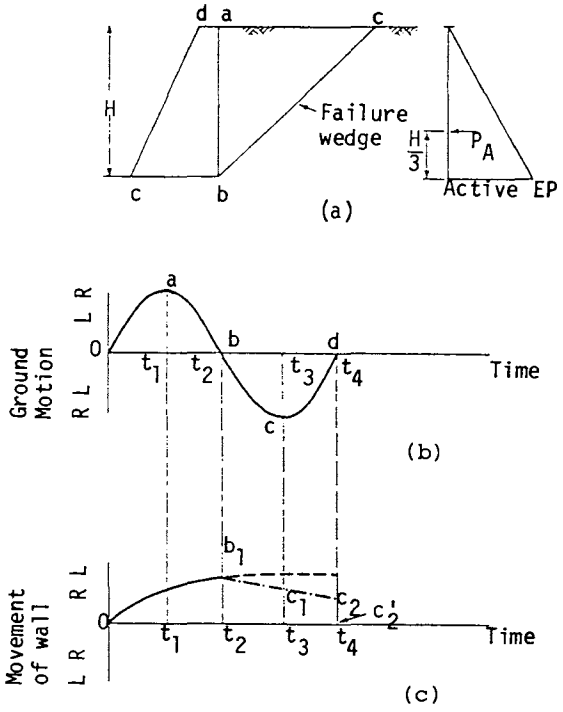

Figure 2. Response of a Rigid Wall to Ground Motion (after Prakash, 1981)

studies in the determination of dynamic earth pressure.

Analysis for c-ϕ Soils

The modified Coulomb's method has been applied only to cohesionless soils. A general solution that can be used to determine total (static and dynamic) earth pressures for a c-ϕ soil has been developed by Prakash and Saran (1966) and Saran and Prakash (1968).

Figure 4 shows a wall with face ab in contact with the soil and vertically inclined at angle α. The soil retained is horizontal and carries uniform surcharge, q, per unit area. The assumed failure surface is vertically inclined at θ through b. If the depth of the tension crack is H_c, let

$$H_c = n(H_1 - H_c) = nH \qquad (6)$$

in which H_1 is the height of the retaining wall, and H the height of retaining wall free from cracks.

In this analysis, only the horizontal inertial force is considered. All of the forces acting on the assumed failure wedge, abcd, are listed in Table 2 along with their horizontal and vertical components.

A summation of the vertical and horizontal components and elimination of the unknown force, 'R', give

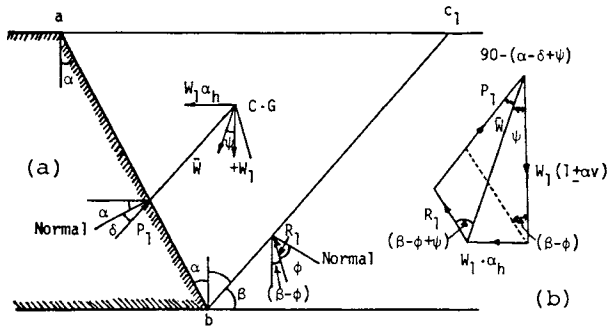

Figure 3. Computation of Dynamic Increment of Earth Pressure by Pseudostatic Method
a) Forces on Soil Mass abc
b) Force Polygon

Table 1. Summary of Analytical Work on Dynamic Earth Pressure

S. No.	Author and Year	Description
1	Sano (1916)	ϕ replaced with $(\phi-\tan^{-1}\alpha_h/1-\alpha_v)$ for use in either Rankine's or Coulomb's theory. Thus a pseudo decrease in ϕ is considered to account for the additional inertial force.
2	Okabe (1924)	Considered failure wedge equilibrium as in Coulomb's theory, with additional inertia forces due to horizontal and vertical acceleration. Analyzed both for cohesionless and cohesive soils.
3	Mononobe (1929)	Rotated the whole cross section by an angle $\psi(=\tan^{-1}\alpha_h/1-\alpha_v)$.
4	Matsuo & Ohara (1960)	Developed for quay wall design. Backfill was considered an elastic two-dimensional body. Total design pressures were given as sum of soil pressures and hydrodynamic pressures.
5	Ishii, Arai & Tsuchida (1960)	Developed for quay wall or retaining wall design, similar to Matsuo and Ohara theory. For fixed wall, soil is assumed as visco-elastic and for moving wall, the soil is assumed elastic but weight of wall is also considered.
6	Kapila (1962)	Modified Culman's graphical construction to account for dynamic forces.
7	Arya & Gupta (1966)	Obtained non-linear distribution of earth pressure by assuming linear variation of horizontal acceleration with depth. Gives unsafe values.
8	Prakash & Saran (1966)	Gave non-dimensional plots for determining dynamic pressures exerted by a c-ϕ soil on retaining walls. Gravity, surcharge and cohesion effects are separately optimized and then superimposed, hence method is conservative. Plane rupture surface below tension crack zone is considered. It was found that the effect due to cohesion is unaltered in dynamic case.
9	Madhav & Rao (1969)	Presented design curves as function of (1) cohesion, (2) angle of internal friction, (3) seismic coefficient, (4) wall friction, (5) inclination of wall back and (6) inclination of backfill. Pseudo-static analysis was used. Direction of resultant inertial force was optimized to get maximum resulting pressures.
10	Prakash & Basavanna (1969)	Gave simple empirical formula for dynamic earth pressure distribution by studying Mononobe-Okabe formula.

Table 1. (Continued)

S. No.	Author and Year	Description
11	Basavanna (1970)	Modified earlier work of Prakash and Basavanna (1969) avoiding the discrepancy that full friction along the rupture surface is mobilized even when the components of body forces parallel and perpendicular to the ground surface were acting separately.
12	Scott (1973)	The soil was treated as a one-dimensional shear beam attached to the wall by springs representing the soil-wall interaction. It was concluded that the pressures and moments are significantly higher than those calculated by Mononobe-Okabe method. The point of application of the earth pressures are in general around 2/3 H above the base.
13	Tazimi (1973)	Used two dimensional wave propagation theory in homogeneous elastic body to determine dynamic earth pressures or walls displaced either in translation or rotation.
14	Jakovlev (1977)	Two approaches used for computation of active and passive pressures (1) based on Coulomb's Theory and (2) based on safe-stress static theory.
15	Aggor & Brown (1973)	Used finite element model of wall-backfill system excited by sinusoidal ground motion. Conclusion: (1) In flexible wall pressure near top is smaller than on rigid wall, (2) Dynamic pressures depend very much on static pressures.
16	Nandkumaran & Johi (1973)	Proposed a method of determining the point of application of dynamic earth pressure. Assumptions are (1) rupture surface already developed, (2) it does not change under earthquake, and (3) no tension cracks on rupture surface. Results are--point of application of dynamic increment is dependent (1) on the geometry of the problem, (2) on the design seismic coefficient and (3) point of application is below the two-third point above the base of the wall.

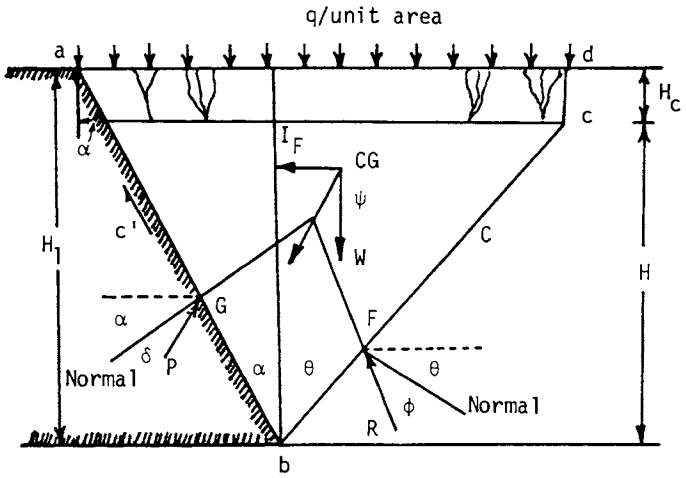

Figure 4. Forces Acting on a Wall Retaining c-φ Soil and Subjected to an Earthquake Type Load (after Prakash and Saran, 1966)

$$P \sin(\beta+\delta) = \gamma H^2[(n+\tfrac{1}{2})(\tan\alpha+\tan\theta) + n^2\tan\alpha] \times [\cos(\theta+\phi) + \alpha h \sin(\theta+\phi)] + qH[(n+1)\tan\alpha + \tan\theta] \times [\cos(\theta+\phi) + \alpha h \cdot \sin(\theta+\phi)] - cH[\cos\beta \sec\alpha + \cos\alpha \sec\theta]$$

in which

$$\beta = (\alpha+\theta+\phi). \tag{8}$$

By introducing the following dimensionless parameters,

$$(Nac)_{dyn} = \frac{\cos\beta \sec\alpha + \cos\phi \sec\theta}{\sin(\beta+\delta)} \tag{9}$$

$$(Naq)_{dyn} = \frac{[(n+1)\tan\alpha + \tan\theta][\cos(\theta+\phi) + \alpha_h \sin(\theta+\phi)}{\sin(\beta+\delta)} \tag{10}$$

Table 2. Computation of Forces Acting on Wedge abcd. (Figure 4)

S. No.	Designation	Vertical Component		Horizontal Component
1	Weight of Wedge abcd (W)	$1/2\gamma H^2(\tan\alpha+\tan\theta)+\gamma nH^2(\tan\alpha+\tan\theta)$ $+1/2\gamma n^2H^2(\tan\alpha)$	↓	---
2	Cohesion cH secθ	cH	↑	cH tanθ →
3	Adhesion c'H secα	c'H	↑	c'H tanα →
4	Surcharge Q	qH [(tanα+tanθ)+nH tanα]	↓	--
5	Soil Reaction	R sin($\theta+\phi$)	↑	R cos($\theta+\phi$) ←
6	Inertial Force I_F	--		$(W+Q)\alpha_h$ ←
7	Earth Pressure P	P sin($\alpha+\delta$)	↑	P cos($\alpha+\delta$) →

and

$$(N\alpha\gamma)_{dyn} = \frac{[(n+\frac{1}{2})(\tan\alpha+\tan\theta)+n^2\tan\alpha][\cos(\theta+\phi)+\alpha_h\sin(\theta+\phi)]}{\sin(\beta+\delta)} \quad (11)$$

one obtains

$$(P)_{dyn} = \gamma H^2(N\alpha\gamma)_{dyn} + qH(Naq)_{dyn} - cH(Nac)_{dyn} \quad (12)$$

in which $(Nac)_{dyn}$, $(Naq)_{dyn}$ and $(N\alpha\gamma)_{dyn}$ are earth pressure coefficients and which depend on α, n, ϕ, γ, and θ.

The values of the earth pressure coefficients in these equations have been determined by optimizing each coefficient. The final equation gives the upper bound of the active earth pressure.

For the static condition, ψ equals zero. Equations 9, 10 and 11 are then changed as follows:

$$(Nac)_{stat} = \frac{\cos\beta\ \sec\alpha + \cos\phi\ \sec\theta}{\sin(\beta+\delta)} \quad (13)$$

$$(Naq)_{stat} = \frac{[(n+1)\tan\alpha + \tan\theta)]\cos(\theta+\phi)}{\sin(\beta+\delta)} \quad (14)$$

$$(N\alpha\gamma)_{stat} = \frac{[(n+\frac{1}{2})(\tan\alpha+\tan\theta) + n^2\tan\alpha]\cos(\theta+\phi)}{\sin(\beta+\delta)} . \quad (15)$$

Maximum values of earth pressure coefficients were also obtained for the dynamic case. It is seen that (Nac) has the same value in the static case. The ratio of the coefficients from the dynamic to the static case may then be defined as

$$\lambda_1 = \frac{(Naqm^*)_{dyn}}{(Naqm)_{stat}} \quad (16)$$

and

$$\lambda_2 = \frac{(N\alpha\gamma m)_{dyn}}{(N\alpha\gamma m)_{stat}} . \quad (17)$$

In Figure 5, (Nac) has been plotted against 'ϕ'. This plot is independent of 'n', and the inclination of the wall, 'α', has been considered from 0° to ± 20°, (Prakash and Saran, 1966; and Saran and Prakash, 1968), $(Naq)_{stat}$ versus ϕ has been plotted for n = 0 and n = 0.2 in Figures 6 and 7, respectively, and $(N\alpha\gamma)_{stat}$ versus ϕ has been plotted for n = 0 and n = 0.2 in Figures 8 and 9, respectively.

It was found that λ_1 and λ_2 are nearly equal and that these values alter slightly with an increase in n. It is therefore recommended that the effect of 'n' on λ_1 and λ_2 be not considered, (Prakash and Saran, 1966; and Saran and Prakash, 1968). Hence, only one value of $\lambda(=\lambda_1=\lambda_2)$ has been plotted in Figure 10, and λ is the ratio of earth pressure coefficients in the dynamic to the static case and increases with increasing α_h.

EXPERIMENTAL STUDIES

Large quantities of experimental data concerning the magnitude of the total (static and dynamic) earth pressure during vibrations have been collected. Many experimental studies have been conducted on small walls to understand their physical behavior. The basic purpose of these earth pressure experiments has been to simulate the strain conditions in the backfill, and thus,

*Subscript 'm' stands for the maximum value of the coefficient.

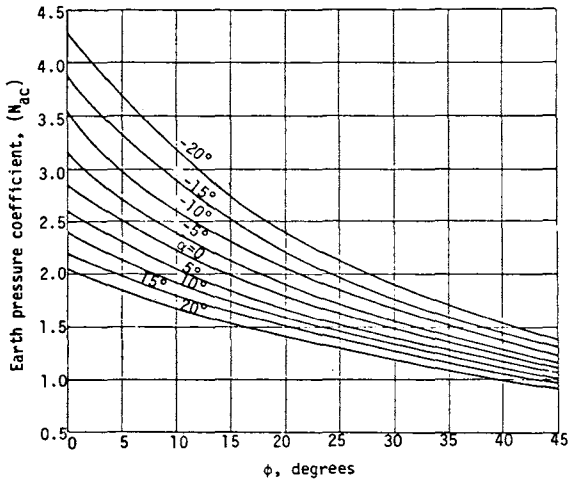

Figure 5. N_{ac} vs ϕ for all Values of n (after Prakash and Saran, 1966 and Prakash, 1968)

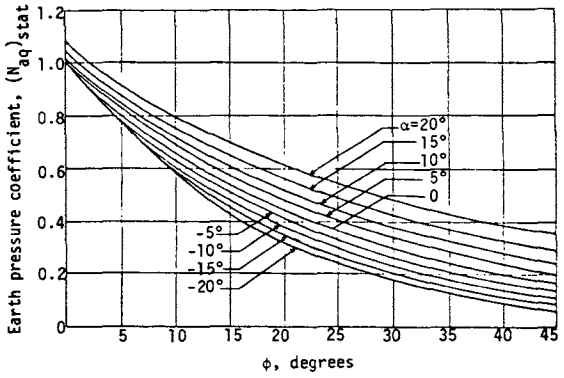

Figure 6. $(N_{av})_{stat}$ vs ϕ for n = 0 (after Prakash and Saran, 1966 and Saran and Prakash, 1968)

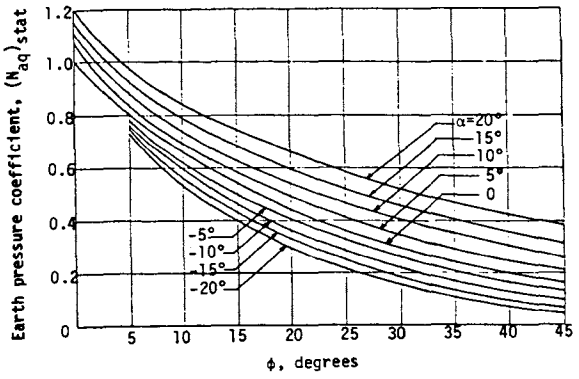

Figure 7. $(N_{aq})_{stat}$ vs ϕ for n = 0.2 (after Prakash and Saran, 1966 and Saran and Prakash, 1968)

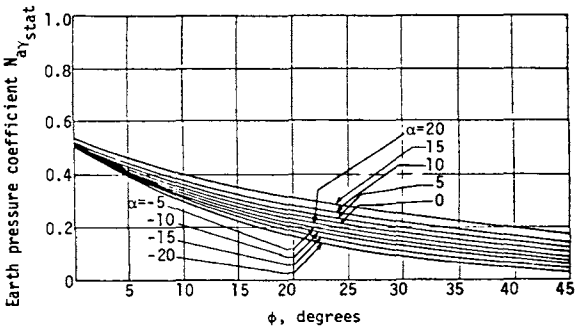

Figure 8. $(N_{a\gamma})_{stat}$ vs ϕ for n = 0 (after Prakash and Saran, 1966 and Saran and Prakash, 1968)

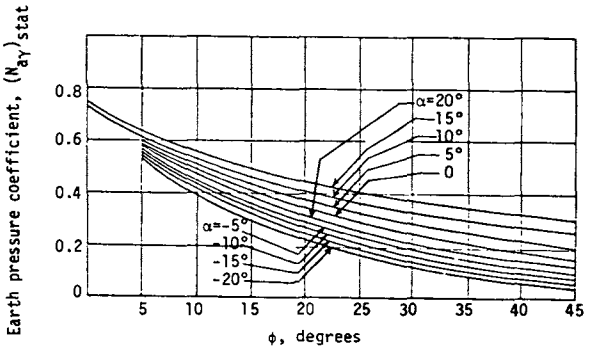

Figure 9. $(N_{a\gamma})_{stat}$ vs ϕ for n = 0.2 (after Prakash and Saran, 1966 and Saran and Prakash, 1968)

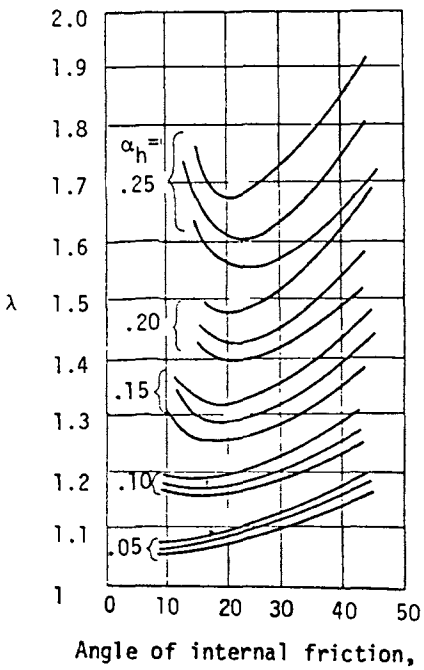

Figure 10. λ vs ϕ (after Prakash and Saran, 1966)

to treat the setup as a small prototype. A fairly comprehensive review of the significant experimental studies has been prepared by Nandkumaran (1973, 1974). Seed and Whitman (1970) and Prakash (1981) have discussed at length some typical studies.

Table 3 lists the pertinent works pertaining to experimental studies. The most significant conclusions that have been derived from these are:

1. The dynamic increment in earth pressure is equal to the one predicted by Mononobe-Okabe's pseudostatic method.

2. Residual pressures after the vibrations have ceased have in some cases been found to be larger than the pressures during vibrations.

3. There is no general agreement on the point of application of the dynamic increment. The height of the incremental dynamic pressure has been observed to vary from 1/3 H to 2/3 H above the base; H being the height of the wall.

It is important that the following questions be answered before the above conclusions can be translated into practice:

1. During an earthquake, the peaks of the ground motion acceleration are not constant. What value of acceleration may be considered for computation of the dynamic earth pressure increment?

Seed and Whitman (1970) recommended that $\Delta P_{dyn} = 1/2\gamma H^2 \Delta_{KAE}$ in which $\Delta_{KAE} = 3/4(\alpha_h g)$.

For a typical nonuniform aperiodic ground motion, what value of $(\alpha_h g)$ may be adopted?

Clough and Fragaszy (1977) found that if 70% of the peak surface acceleration is used in Mononobe-Okabe analysis, good correlation is obtained between predicted and actual failure.

2. A center of pressure at a higher elevation than those currently used will cause larger moments on the base and result in more severe loading conditions. Hence, what would be a realistic position for the center of pressure?

An elaborate testing program to determine total earth pressure and the center of dynamic increment was undertaken at Roorkee University in 1970. The salient features of this investigation are mentioned here, because it has not been extensively reported in the United States.

In this program, tests were conducted on three walls as follows: 1) 1m high flexible wall, 2) 1 m high rigid wall, and 3) 2m high rigid wall.

1m High Flexible Wall

Considering high retaining walls, the strain in the backfill is most likely to be due to flexural bending of the wall because of the possibility of extremely rigid foundations. However, any strain in the foundation soil will result in the rotation and translation of the wall as a body. If the foundation is not very rigid, the deformation due to rotation is likely to obliterate any deformation due to bending.

In a model study for determining the effect of dynamic earth pressures on wall deformations, it is not advisable to introduce flexural bending deformation and a movement of the wall as a body simultaneously. The solution to this problem is to conduct separate tests on two walls, one that is subject to bending deformations only and the other that undergoes deformations as a rigid body (Krishna et al., (1974). Therefore, the flexible wall which was rigidly held at its base, would experience deformations due to bending only.

Test Setup

Test Bin. A large bin, 5.2m x 2.8m x 1.2m high mounted on a shaking table that could be set into motion by the impact of a pendulum was used at Roorkee University. The size of the shake table made it possible to use a fairly large wall for the tests. This reduced the number of errors that are inherent in small apparatus (Fig. 11).

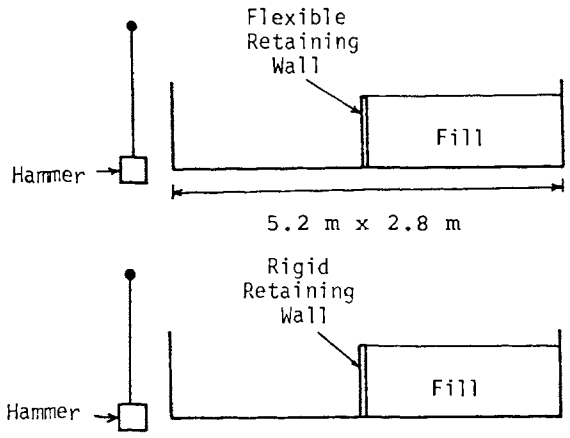

Figure 11. Large Shake Table Used for Tests on Retaining Walls at Roorkee

The Wall. A high cantilever wall on a rigid foundation can best be represented in a model by a metal wall rigidly fixed to a base and having sufficient thickness to permit comparable deflections so as to induce strains of similar order in the backfill (Fig. 12a).

Thus, it is clear that the problem of modeling the wall is that of obtaining comparable deflections. Because the wall is designed for active earth pressures, comparable deflections in the model and the prototype can be obtained by considering the deformations required for the development of active conditions.

Terzaghi (1936) gave approximate quantitative values of the amounts of yield needed for two types of active cases (arching active and totally active) in the case of one typical dense sand. The values are:

1. If the mid-height point of the wall moves outward a distance roughly equal to one-twentieth of 1% of the wall height, an arching active case is attained.

2. If the top of the wall moves outward an

Table 3. Summary of Experimental Work on Dynamic Earth Pressures

S. No.	Author and Year	Description
1	Matsuo (1941)	Used box mounted on shake table. Found dynamic component of pressure to act at 2/3 H above base (as against 1/3 H in Mononobe-Okabe analysis).
2	Jacobsen (Tennessee Valley Authority, 1951)	Used shake table, pressures were measured using dynamoters restraining the wall model. Results agree reasonably with Mononobe-Okabe analysis, but dynamic component of pressure is found to act at upper third point of wall.
3	Matsuo & Ohara (1960)	Conducted tests on fixed and movable walls with dry sand on shake table. Pressures monitored using piston type pressure cells. Period of vibration was 0.3 sec. Results were--(1) Fixed walls--amplitude of pressure change is large at H/2. (2) Movable walls--maximum amplitude of pressure decreases with displacement below certain value of displacement.
4	Ishii, Arai & Tsuchida (1960)	Used shake table to test three setups. Period of vibration was 0.3 sec. Model of gravity wall was also tested. Results were (1) up to acceleration = 500 gals--no marked change in earth pressures, (2) for acceleration between 500-800 gals, lateral pressure increases and settlement of sand occurs, (3) for acceleration beyond 800 gals, dry liquefaction is observed but settlements became smaller, (4) phase difference up to half the period was observed between the table motion and the pressures in the movable wall, (5) maximum pressure is equal to or lower than Mononobe-Okabe pressure, (6) dynamic pressure distribution is bowshaped.
5	Murphy (1960)	Conducted tests on a solid rubber model of a gravity wall. Conclusion is that slip surface under dynamic load is much flatter than that in static case.
6	Niwa (1960)	Conducted tests on a 3m high concrete retaining wall excited by an earthquake generator. The amplitude of vibration of the wall was split into translation and rocking components.
7	Ichihara (1965)	Measured pressures and moments created by a backfill on a model wall when the whole system is vibrated. Conclusion was that movement of wall causes reduction in pressure and moment.
8	Aliev, Mamedv & Radgabova (1973)	Used a different approach using similitude and centrifuge technique to increase the acceleration and resulting seismic pressures were monitored. Field tests on two walls (one founded on rock, other on sandy cushion) were also carried. Result was that introduction of sand cushion below retaining walls considerably reduces dynamic earth pressures. A definite conclusion was not made.
9	Nandkumaran (1973, 1974)	Measured dynamic increment of earth pressure on three small sized walls--1m high flexible and rigid walls and 2m high rigid wall. Correlated dynamic increment with peak ground velocity and recommended a procedure for computing displacements of rigid walls in translation.
10	Sim and Berrill (1979)	Shaking table tests of a model gravity retaining wall are described. The tests were designed to check the validity of the simple analytical model of wall behaviour proposed by Richards and Elms (1979). The results show that the wall translates outwards in a stepwise fashion under strong shaking as predicted by the analytical model.

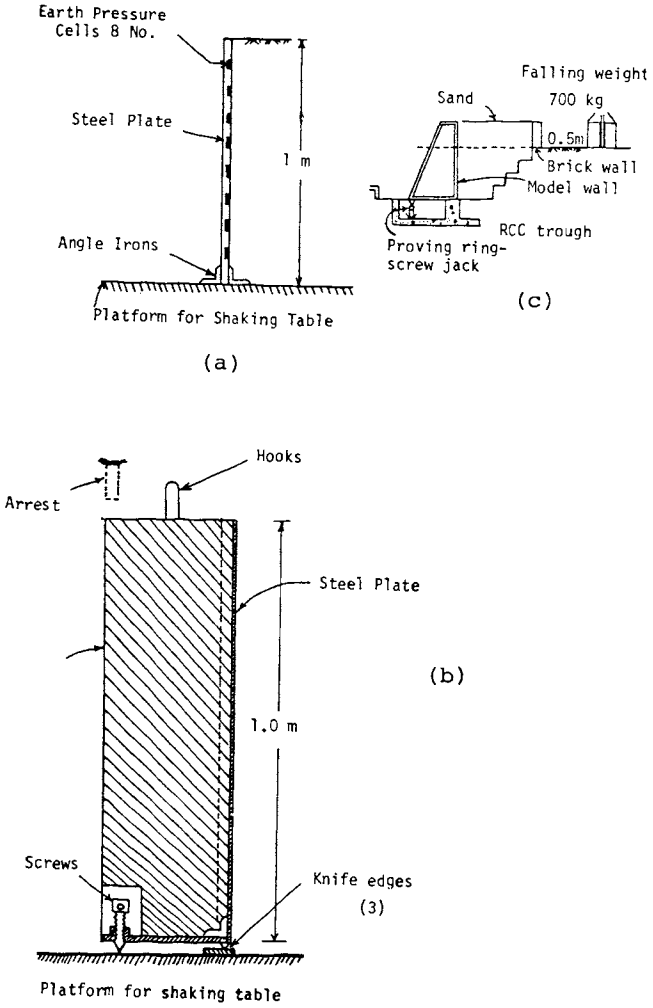

Figure 12. Sections of Walls (a) 1m flexible, (b) 1m rigid, (c) 2m rigid

amount roughly equal to one-half of 1% of the wall height, the fully active case is attained.

The above values are valid only for rigid walls, but a reasonable modification of these for flexible walls seems to be the best way of obtaining the thickness of the model wall. Accordingly, it has been arbitrarily assumed that the deformation of the mid-height of the wall is one-fourth of 1% of the height of the wall for active conditions (Krishna et al., 1979).

To have a fairly large height to length ratio for the wall, a wall height of 1.0m was adopted. The thickness of this cantilever for deflections of 1/400 times the height at mid-height was found to be 1.0 cm. For this computation, the load on the wall was taken as a linearly varying load computed from Rankine's theory.

Pressure Measurements. Eight pressure cells were fabricated and used to measure the pressures in static as well as dynamic conditions (Nandakumaran, 1973).

Soil. Air dried, clean, Ranipur sand was used in the experiments. The salient properties of the sand (Fig. 13) were:

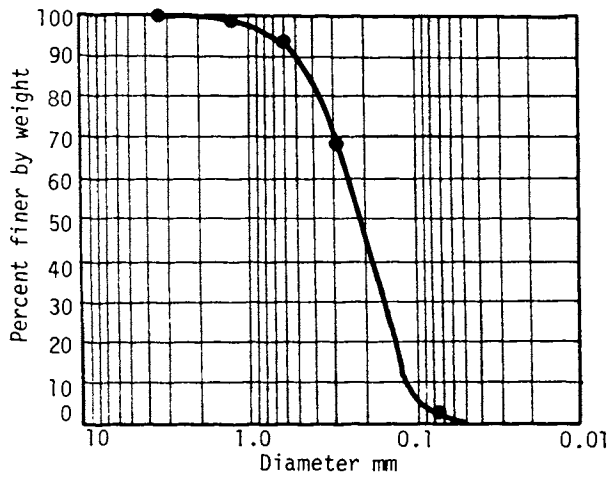

Figure 13. Grain Size Distribution Curve of Ranipur Sand (after Krishna et al., 1974)

a. Soil type: SP (poorly graded sands with little or no fines according to Indian Standards Classification)
b. Uniformly coefficient = 2.10
c. Effective size, D_{10} = 0.13mm
d. Specific gravity of soil solids, S_s = 2.66
e. Relative density at the test condition = 56%
f. Grain size distribution of sand is shown in Figure 13.

The minimum and maximum void ratios of the sand were determined to be 0.575 and 0.86 respectively.

Ranipur sand has a fairly high shearing resistance. The angle of internal friction is 38.5° at a relative density of 31.5% and 42° at a relative density of 70.25% (Narain et al., 1969). The value of the angle of internal friction in the test condition was 40°.

Sand Placements. Sand was placed in a tank in 10cm layers. Each layer was compacted by placing a wooden plank 90.0 x 30.0cm on the surface of the sand and striking the plank with six blows of a wooden mallet. Five calibrated tins were kept during the filling of each layer, and the density of the sand was determined after each layer was completed. It was observed that this method gave the same reproducible densities throughout the deposit.

Test Procedure and Test Results. The zero readings of all the eight pressure cells, all the eight strain gages, and the five dial gages were taken, and then the wall was backfilled with the sand. The final readings of all the cells, strain gages, and the dial gages were taken. The differences between the final readings and the initial readings furnished the data to compute the earth pressures, bending moments, and deflections at various elevations of the wall.

During a single impact of a pendulum, simultaneous records of the acceleration of the table, acceleration of the wall, and increase in earth pressure at one elevation were made. By imparting identical shocks to the table eight times,

the increase in pressures at each of the elevations, was obtained, and, hence, the pressure distribution diagram was constructed. This was necessary, because only three channels were available for recording. Two channels were used for recording the acceleration, and one for recording the earth pressure at each elevation.

The earth pressures obtained from tests in which four different table accelerations were employed are listed in Table 4. Figure 14 shows the pressure diagram with depth for static, dynamic, at-rest ($k_o = 1 - \sin\phi$), and active ($k_a = 1-\sin\phi/1+\sin\phi$) conditions.

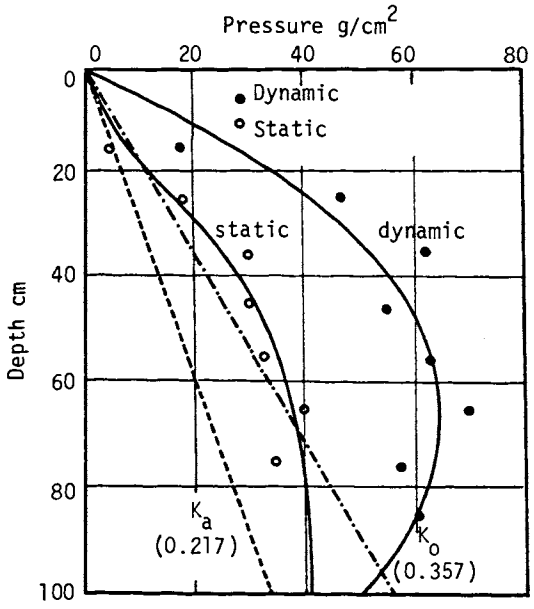

Figure 14. Static and Dynamic Earth Pressure Distribution Behind 1m High Flexible Wall (after Prakash and Nandkumaran, (1979)

Similar data were obtained for other tests (Nandkumaran, 1973). From Figure 14, it can be seen that the initial conditions for the dynamic tests were not active but some state between at-rest and active. This condition is nearly equal to the at-rest pressure condition posulated by Jaky (1948). Because of the similarity of wall deformations and backfilling procedures in the model and in practice, these initial conditions are likely to hold good for a cantilever retaining wall on rigid foundations. The impact loads applied on the wall had to have a higher magnitude of acceleration than is generally considered suitable because of the short duration of the loads. As is well understood, the magnitude of earth pressures is inevitably a function of the strain in the backfill, which in turn is dependent on the movement of the wall. Therefore, to simulate realistic loading conditions, the magnitude as well as the duration of the dynamic loads become the two most important criteria to be adopted. The damage suffered during an earthquake depends upon the peak particle velocities induced in the ground. The peak ground velocity induced during the impacts was of the order of 17cm/sec which is comparable with the ground motion velocities during some earthquakes. The correlations obtained for the dynamic earth pressures from the present studies may therefore be considered representative for the actual cases.

The dynamic increment and peak ground acceleration for flexible and rigid walls are plotted in Figure 15. Theoretically computed values of the dynamic increment as well as those obtained by the Mononobe-Okabe method are also plotted. The peak acceleration values were so high that it was not possible to compute the dynamic increment in earth pressure (Prakash and Saran, 1966).

Because it is the energy or the peak ground velocity that is important in seismic phenomena, the time vs acceleration data of input ground motion (table motion) was integrated, for each test, and a plot of the coefficient of the dynamic increment, c_p, which is defined as $c_p = \frac{\text{dynamic increment}}{1/2\ \gamma\ H^2}$, versus peak ground velocity is shown in Figure 16. The results of the theoretical computation (from the Mononobe-Okabe method) for the peak acceleration, as in the tests and the arbitrary periods of motion of 0.25 sec, 0.3 sec, and 0.35 sec, are also plotted in this figure. It can be seen that the results lie very close to the theoretical curve of a 0.3 sec period. This aspect is discussed further. An interpretation of the static test results is presented elsewhere (Nandkumaran, 1973; Krishna et al., 1974.

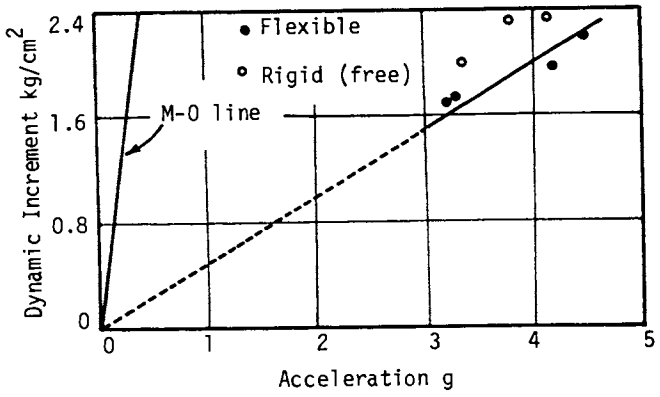

Figure 15. Dynamic Increment vs Peak Ground Acceleration in 1m High Walls (after Prakash and Nandkumaran, 1979)

During the shock loading, the dynamic increment (the increase in pressure occasioned by the shock) along the height was measured and is as shown in Figure 17, no rupture developed in the backfill, although the wall moved out, thereby indicating that the pressures did not drop to active values during any part of the test. Therefore, it is reasonable to assume that the dynamic increment is the result of the soil-structure interaction during the shocks and, hence, may be valid even if the initial conditions were different, than the state of active equilibrium behind the wall.

Another point of interest was the gradual outward movement of the wall. This can be explained in terms of the different magnitudes of walls resistance to motion towards and away from the backfill. The former consists of the stiffness of the wall and passive pressure from the backfill, whereas the latter is only the stiffness of the wall minus the active earth pressure on the wall and is much smaller. This may be sufficient reason to assume that the wall does not

Table 4. Particulars of Test Data on 1m Flexible Wall*

Test No.	Total Static Pressure g/cm of Wall	Static E.P. Coefficients	Point of Application Above Base cm	Acceleration in Test (Peak) g	Total Dynamic Increment g/cm of Wall	Pont of Application Above Base cm	Dynamic Increment / Static Pressure
1	2658.0	0.3343	37.60	4.29	1961.0	54.65	0.750
2	2798.7	0.3520	36.00	3.32	1659.5	50.30	0.604
3	2641.3	0.3322	34.25	3.34	1680.0	50.05	0.646
4	2697.0	0.3392	36.00	4.55	2177.0	48.30	0.807

*After Krishna et al., 1974 and Prakash and Nandkumaran, 1979.

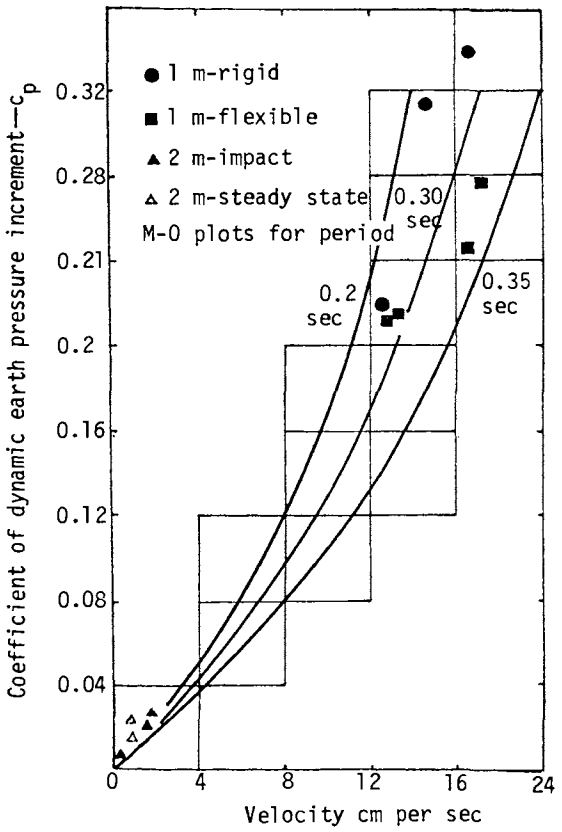

Figure 16. Peak Ground (Table) Velocity vs Dynamic Increment of Earth Pressure (after Prakash and Nandkumaran, 1979)

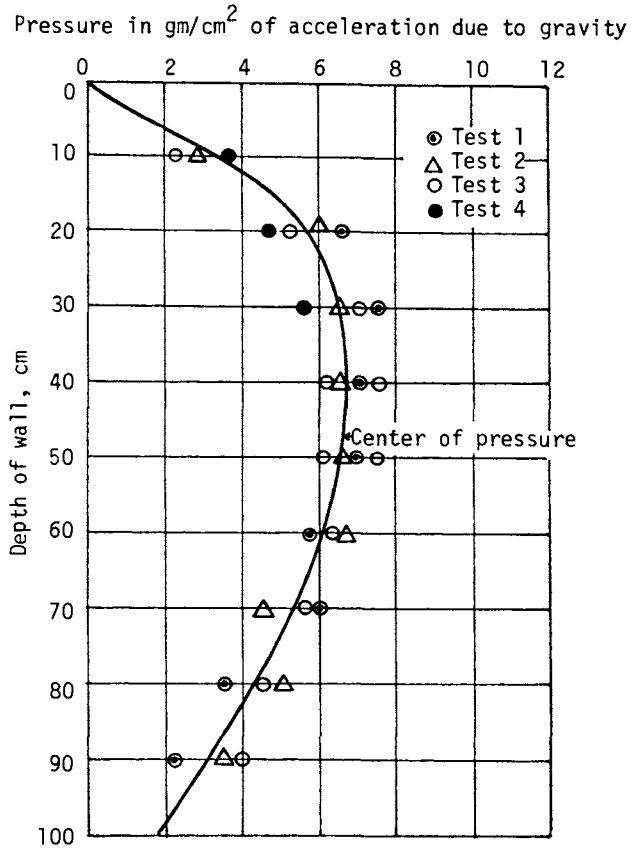

Figure 17. Distribution Diagram of Dynamic Increment per Unit of Acceleration Due to Gravity with Height in Flexible Wall (after Krishna et al., 1974)

vibrate, and so the pressures do not become magnified on account of posisble resonance during earthquakes. Because of the above two reasons, the dynamic increment distribution as observed during tests is realistic for design purposes.

1m High Rigid Wall

The cross section of the 1m rigid wall is shown in Figure 12b. Eight cells were used to measure the earth pressures. The wall was not permitted to move during backfilling. Active conditions were generated by subsequently rotating the wall. The test bin was then excited, and the dynamic increment of pressure was recorded with height as for the flexible wall. Two types of tests were performed. In one series (Tests 1, 2 and 3, (Table 5), the top of the wall was not allowed to move, whereas in Tests 4, 5 and 6, the wall was free to move during the dynamic loading. The data of this test series that are of practical importance are plotted in Figure 15. The plots of the peak ground velocity and coefficient of dynamic increment for the tests on rigid walls are plotted in Figure 16. The points lie close to the theoretical line with the period of 0.3 sec. The peak ground velocities in this test series are comparable to those in the tests on 1m flexible wall.

It was therefore found that for rigid walls the dynamic pressure increment also has a unique correlation with peak ground velocity as was the case for the flexible wall. The distribution of the dynamic increment along the height of the wall in one of the tests is shown in

Table 5. Particulars of Test Data on 1m High Rigid Wall

Test Series	Table Acceleration g	Dynamic Pressure gm/cm	Point of Application Above Base cm	Remarks
1	4.21	2647.0	41.5	No wall movement
2	3.71	2469.5	36.4	No wall movement
3	3.31	1716.5	40.6	No wall movement
4	4.71	2394.0	44.3	Wall moves during shocks
5	3.71	2377.6	37.4	Wall moves during shocks
6	3.31	1986.5	41.2	Wall moves during shocks

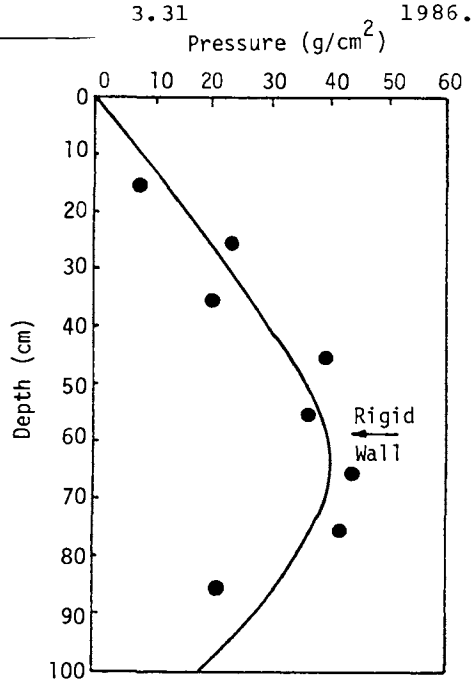

Figure 18. Dynamic Earth Pressure Distribution in Rigid Walls (after Prakash and Nandkumaran, 1979)

Figure 18. It can be seen that the pressure increases linearly downward from the top of the wall and reaches a maximum value at an elevation of nearly 65% of the height from the top, where there is a decrease in the pressures. Similar trends were observed in all the six test series. The magnitude and the center of pressure in all the tests are tabulated in Table 5 (Prakash and Nandkumaran, 1979). Thus the center of dynamic pressure increment may be taken at 0.45 H above the base.

2m High Rigid Wall

The cross section of the wall is shown in Figure 12c. Although the peak accelerations employed in the two types of tests already described could be considered as large, the fall of a concrete block in this case produced accelerations of the order of 0.3g. However, even in this case, it was observed that both under impact loading conditions and the steady state vibrations the pressures had not been correctly estimated by the Mononobe-Okabe theory. An attempt was, therefore, made to see the validity of the correlation between the peak velocity and the dynamic increment previously established. The test results are given in Table 6, and the values are plotted in Figure 16.

The most significant conclusion to be drawn from this study is that the dynamic increment in active earth pressure has a unique correlation with the peak ground velocity. For a given problem, a seismogram can be selected, and from the peak ground velocity, V_{max}, for this ground motion, the seismic coefficient, α_h, for computing dynamic increment can be obtained by using

$$\alpha_h = V_{max} \frac{2\pi f}{g} \qquad (18)$$

in which f is the frequency corresponding to an arbitrary selected period of 0.3 sec, and g is the acceleration due by gravity.

POINT OF APPLICATION OF DYNAMIC INCREMENT

The location of the center of pressure determines the magnitude of the overturning moment. It is more or less accepted that the static active as well as the at-rest pressures vary hydrostatically along the height of a wall.

The solution of Mononobe-Okabe is based upon Coulomb's theory. The earth pressure distribution in the static case of walls with simple boundary conditions (plane walls and horizontal fill) is hydrostatic. Therefore, for the dynamic case, the distribution is also hydrostatic, but a large amount of experimental data on small sized walls indicates that a parabolic distribution of incremental earth pressure is caused by dynamic action. Thus, the center of incremental pressure is above the third point (H/3) from the base.

Matsuo (1941) and Jacobsen (1951) found in their experiments that the center of dynamic incremental earth pressure is, however, 2/3 H above the base. This would be so if the maximum stress intensity occurs close to the top and is near zero at the base, or some similar distribution.

In the test data of Matsuo and O'Hara (1960), Ishi et al., (1960), and Murphy (1960), the dynamic earth pressure distribution was found to be parabolic with the maximum ordinate near mid-height, therefore the center of pressure was above the lower third point above the base.

The position of the resulting (static and dynamic) center of pressure depends upon the amount of wall movement and the way in which the movement occurs (Seed and Whitman, 1970); usually it is located at a height slightly greater than H/3 above the base.

Table 6. Peak Ground Velocities and Coefficient of Dynamic Increment for 2m High Wall

Peak Ground Velocity cm/sec	Coefficient of Dynamic Increment	Point of Application of Dynamic Increment As % H Above Base	Remarks
0.56	0.00322	59.4	
0.84	0.00623	61.0	
1.12	0.01052	57.3	Impact Load
1.4	0.01710	53.6	
1.68	0.02622	51.4	
0.2	0.002	--	
0.55	0.0065	--	
0.85	0.011	--	Steady State
1.05	0.015	--	

Prakash and Basavanna (1969) stressed the fundamental deficiency in Coulomb's theory and, hence, in the Mononobe-Okabe formula that for a rough wall the equilibrium conditions are not satisfied if hydrostatic pressure distribution is assumed. Therefore, by considering failure along the face of the wall and on a plane surface in the backfill, it was established that the distribution of earth pressures is similar to the distribution of the soil reaction on the rupture surface. Then the equilibrium of the assumed rupture wedge was examined, and the equations for the active pressure components as well as the moments of all the forces about the heel of the wall were worked out. For establishing the actual rupture wedge, the earth pressure was maximized as a function of the rupture angle, and the case of a translating wall was solved. For a wall failing by overturning, the moments were maximized to obtain the actual rupture wedge. The height, ha, of the resulting force for tilting and sliding walls is given by

$$ha = c_{ha} \cdot H/3 \qquad (19)$$

The values of c_{ha} for sliding and tilting walls are plotted in Figure 19.

Basavanna (1970) who modified the earlier work of Prakash and Basavanna (1969), assumed that full friction along the rupture surface is mobilized even when the components of the body forces parallel and perpendicular to the ground surface act separately. This discrepancy was avoided, and a new value of c_{ha} (Fig. 20), was obtained.

Scott (1973) treated soil as a one-dimensional shear beam attached to a wall by springs representing the soil-wall interaction. Different cases, such as 1) constant values of shear modulus, density, and spring constant and 2) constant values of density and spring constant but with the shear modulus increasing parabolically with depth, were considered both for fixed walls and flexible walls. A torsion spring was used to represent the rotation and stiffness at the base. It was concluded that the pressures and moments are significantly higher than those calculated by the Mononobe-Okabe method. The point of application of the earth pressures were determined to be generally around 2/3 times the height of the wall above its base. He maintained that observation of the rupture that occurs in the soils behind retaining walls during earthquakes is essentially a post-failure phenomenon, because

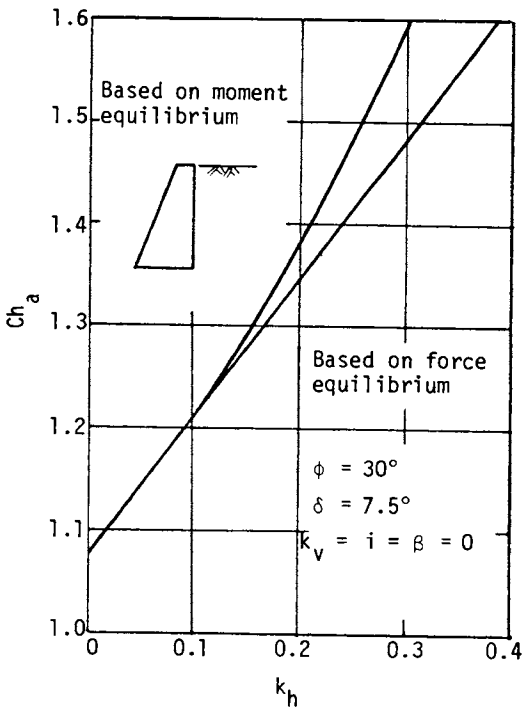

Figure 19. Values of C_{ha} Based on Moment and Force Equilibrium Conditions (after Prakash and Basavanna, 1969)

the walls move out under larger pressures than those derived through use of the Mononobe-Okabe formula, and this displacement causes the development of a rupture in the backfill.

Nandakumaran and Joshi (1973) assumed that 1) the same failure surface occurred in the static and dynamic cases and 2) that there is no tension on the rupture surface. They also established the equilibrium of seismic forces by superposing the dynamic increment on the static forces. The point of application of dynamic pressures was found to depend on the geometry of the problem and the design seismic coefficient, but in general they determined that it is below the two-third point from the base of the wall. Figure 21 shows a plot of the height of the point of earth pressure application above the base of a wall in a typical case.

Woods (1975) theoretically determined the point of application of dynamic earth pressure for an assumed elastic soil to be at approximately midheight.

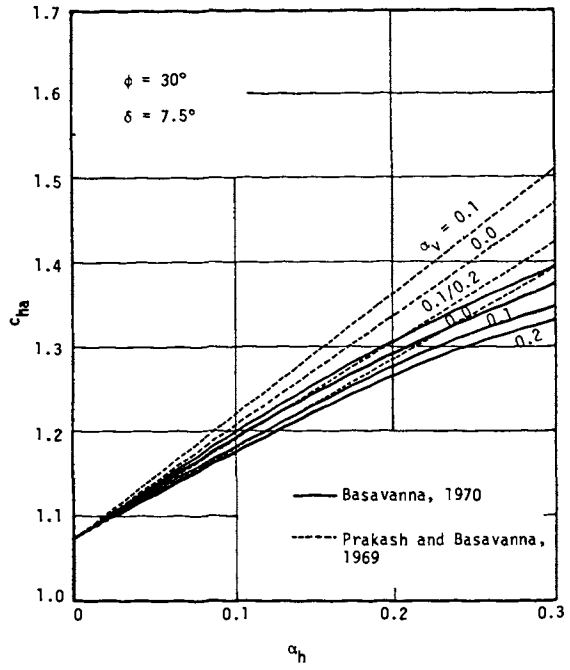

Figure 20. α_h versus $C_{h\alpha}$ (after Basavanna, 1970)

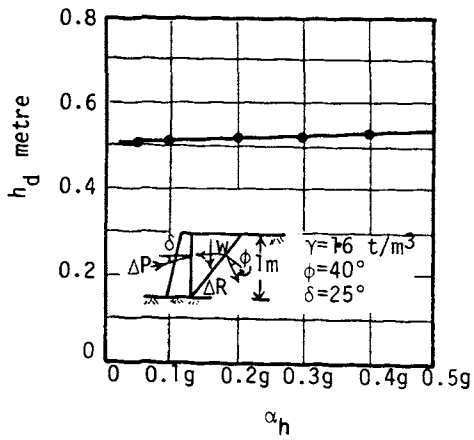

Figure 21. α_h Versus Height of Centroid of Dynamic Increment (after Nandakumaran and Joshi, 1973)

Small scale tests on walls that were reported by Nandkumaran (1973) and Prakash and Nandkumaran (1979) show that the center of pressure of the dynamic increment lies at 0.55 H above the base in flexible wall and 0.45 H above the base in rigid wall.

The above discussion brings out the following significant points:

1. The static pressure distribution is hydrostatic.

2. The magnitudes of pressure are active (Coulomb's or Rankine) if adequate deformation (or strain) in the backfill occurs after it has been placed.

3. The dynamic increment in earth pressure acts at 0.55 H from the base in flexible walls and 0.45 H above the base in rigid walls.

DYNAMIC PASSIVE PRESSURES

The question of dynamic passive pressures has received little attention in the published literature. Coulomb's theory is modified by the pseudostatic approach as for the active condition, and the following expression for total passive pressure, (static + dynamic) is obtained:

$$P_p = \frac{1}{2}(K_p)_{dyn}\,\gamma H^2 \qquad (20a)$$

in which

$$(K_p)_{dyn} = \frac{(1+\alpha_v)\cos^2(\phi+\alpha-\psi)}{\cos\psi\,\cos^2\alpha\,\cos(\delta-\alpha-\psi)} \times \left[\frac{1}{1-\left\{\frac{\sin(\phi+\delta)\sin(\phi+i-\psi)}{\cos(\alpha-i)\cos(\delta-\alpha+\phi)}\right\}^{1/2}}\right]^2 \qquad (20b)$$

in which

H = height of the wall
α = inclination of the wall from the vertical
i = inclination of uniform surcharge from the horizontal
ϕ = angle of internal friction of the soil
δ = angle of wall friction
α_h = horizontal seismic coefficient
α_v = vertical seismic coefficient

$$\psi = \tan^{-1}\frac{\alpha_h}{1+\alpha_v}$$

An earthquake reduces the passive pressure from the static value. Thus, the dynamic component of the total passive pressure is in fact the decrement $(-\Delta P_p)_{dyn}$.

Terzaghi and Peck (1967) demonstrated that static passive earth pressures increase rapidly with increasing values of the angle of wall friction. However, if δ is greater than $\phi/3$, the surface of sliding is strongly curved. Therefore, the error occasioned by Coulomb's assumption of a plane surface increases rapidly. For $\delta = \phi$, it may be as great as 30%. It is reasonable to believe that the corresponding errors in dynamic earth pressures may also be as great. Terzaghi (1943) recommended the use of the general wedge theory to compute static passive earth pressures. Shields and Tolunay (1973) and Basudhar and Madhav (1980) applied the method of slices to compute static passive earth pressures. Corresponding analyses for dynamic earth pressures have not yet been developed (1981).

Sabzeveri and Ghahramani (1974) used an incremental approach to the dynamic analysis of the passive earth pressure problem in which an initially rough vertical wall is considered to move with different values of acceleration with a dry loose sand. Three types of movement, 1) translation, 2) rotation about the top point, and 3) rotation about the toe, were considered. The initial condition in the analysis was "at rest", i.e., k_o condition, and the soil medium was assumed to be rigid plastic.

Numerical computations of the normal stress distribution along the height of the wall 22.5 cm high, for the values of wall rotation (θ_ω) of 1° and 0.25° and for the different values of horizontal acceleration show that the passive earth pressure increases with acceleration. This is apparently contrary to the physical conditions that occur in retaining walls. Also, the meaning of the angle of rotation, θ_ω, in a translating wall has not been explained.

Very few investigations have been made of the dynamic passive pressures and displacements of walls towards a fill when acted upon by forces at the top that result in rotations of the walls about the top or bottom.

Ichihera et al., (1977) investigated the passive earth pressure acting on the front of anchored bulkheads. A specially designed large scale soil bin with a movable wall was developed in their laboratory. A large quantity of clay which was taken from the port of Nagoya was consolidated and allowed to swell in the bin. During translational or rotational inward wall movement, the normal and tangential components and applied point of the resultant force on the wall and lateral earth pressure in the clay were measured. The deformation of the clay adjoining the wall was also investigated. Influence of types of wall movement on the characteristics of the earth pressure and deformation of the clay was investigated, and the test results were compared with the calculated ones based on the conventional method. It was concluded in practical application that the passive earth pressure calculated by the Sokolovski method for the case of $c_a = 2/3\ c_u$ may be applied to the anchored bulkhead.

Jakovlev (1977) has derived several expressions for active and passive pressures under earthquake conditions. Two approaches are described. The first method is based on Coulomb's theory and is used to determine the active pressure and the inclination of the slip surface. The second method is based on safe-stress static theory and is used to compute dynamic active and passive pressures. Both of these methods include surcharge effects.

DISPLACEMENT ANALYSIS OF RIGID RETAINING WALLS

There are three methods of computing displacements of retaining walls, 1) Newmark's Approach, 2) method for computing displacements in translation and 3) method for computing displacements in rotation. All three methods will now be described briefly.

Newmark's Approach

Newmark (1965) proposed a basic procedure for evaluating the potential deformations that would be experienced by an embankment dam shaken by an earthquake. In this important development, he envisaged that slope failure would be initiated and movements would begin to occur if the inertial forces on the potential slide mass were large enough to overcome the yield resistance and that the movements would stop when the inertial forces were reversed. Thus, by computing an acceleration at which the inertial forces become sufficiently high to cause yielding to begin, as shown in Figure 22 and integrating the effective acceleration on the sliding mass in excess of this yield acceleration as a function of time (Fig. 23), velocities and ultimately the displacements of the slide mass could be evaluated.

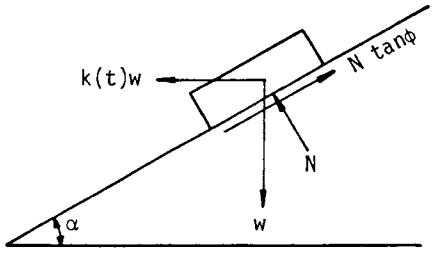

Figure 22. Forces on Sliding Block (after Newmark, 1965)

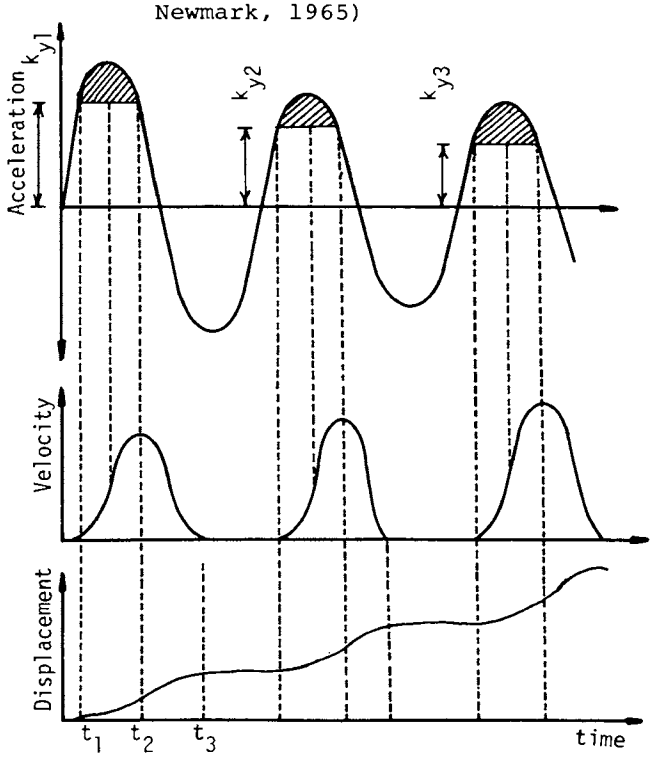

Figure 23. Integration of Effective Acceleration Time History to Determine Velocities and Displacements (after Newmark, 1965)

Newmark's analysis is based essentially upon the rigid plastic behavior of materials (Fig. 24). According to this assumption, the deformation is zero till failure--corresponding to the sliding of the block in Figure 22 occurs.

Although the above method was developed for a sliding analysis of dams, it has been used to compute the displacements of retaining walls.

In Eq. 5, sine (ϕ-ψ-i) appears in the radical of the expression for P_{total}. When this becomes negative no real solution is possible,

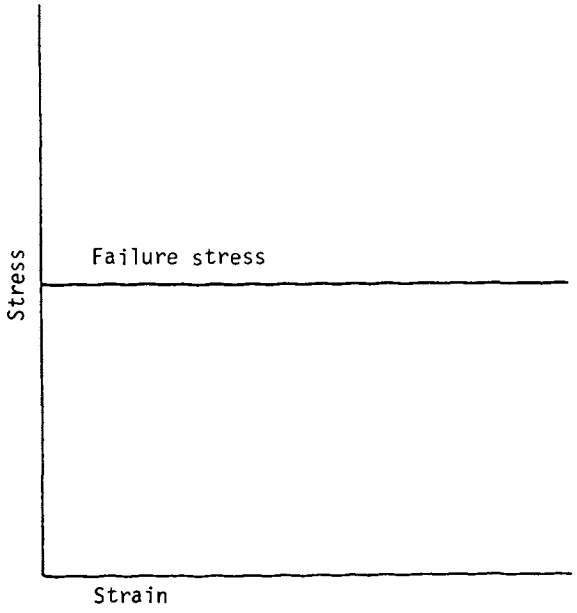

Figure 24. Rigid Plastic Stress Strain Behavior of a Material

corresponding physically to no possibility of equilibrium (as in the static case for slope stability when $i = \phi$ (Richard and Elms, 1979, and Prakash and Saran, 1966). When this term is zero the thrust is a maximum. Thus we have the limiting condition

$$\phi - \psi - i \geq 0 \tag{21a}$$

This may be regarded as giving a limit to the acceleration that can be sustained, regardless of the nature of the retaining wall. For a horizontal backfill, this criterion becomes

$$\psi \leq \phi \tag{21b}$$

or

$$\alpha_h \leq (1 - \alpha_h)\tan\phi \tag{21c}$$

From the above inequality a critical value of horizontal acceleration has been defined (Richards and Elms, 1979).

$$(\alpha_h)_{cr} = (1 - \alpha_v)\tan\phi \tag{22a}$$

and

$$\tan\psi = \frac{(\alpha_h)_{cr}}{(1-\alpha_v)} = \tan\phi \tag{22b}$$

The relative displacements of a wall can be easily calculated from any given earthquake record, if its acceleration time history and sliding cut-off acceleration $(\alpha_h)_{cr}$ are known. Figure 25 gives the acceleration and velocity plots of a soil and wall for the El Centro 1940 N-S record in which the cut-off acceleration coefficient, α_h, is 0.1. The corresponding

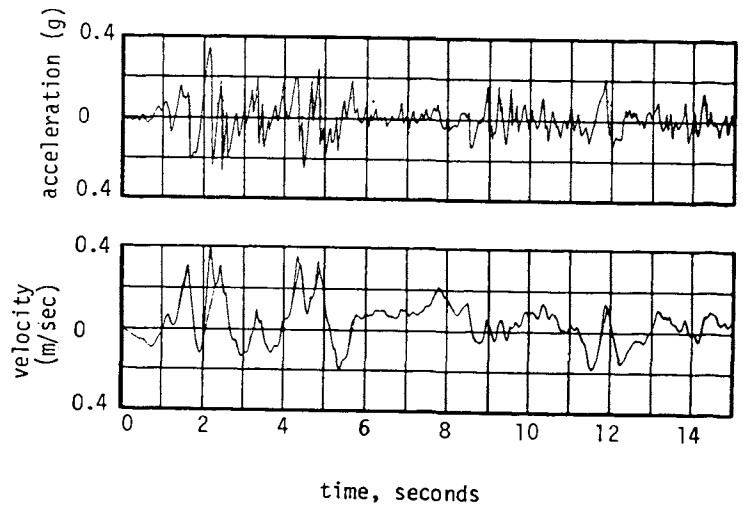

Figure 25. Acceleration and Velocity Time Histories for Soil and Wall, El Centro 1940 N-S; Limiting Wall Acceleration = 0.1g (after Richards and Elms, 1979)

displacement trace is shown in Figure 26. The maximum displacement is about 3 in. (80 mm). Displacements obtained by repeating the analysis for different values of α_h are shown in Figure 27.

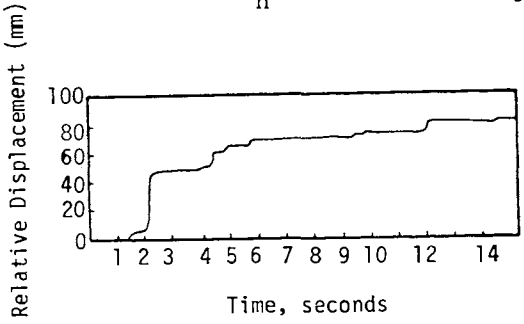

Figure 26. Displacement Time History of Wall Relative to Soil, El Centro 1940 N-S; Limiting Wall Acceleration = 0.1g (after Richards and Elms, 1979

Newmark (1965) analyzed four different earthquakes, and in order to compare the displacement characteristics of the results, he scaled the records in each case to a maximum accleration of 0.5g and a maximum velocity of 30 in./sec. Franklin and Chang (1977) extended this work and analyzed 169 horizontal and 10 vertical corrected accelerograms as well as several synthetic records; they followed Newmark in scaling the records to 0.5g and 30 in./sec and in plotting the standardized displacements. The plots of standardized displacements are particularly interesting in that, although there is some correlation with magnitude, the character of the displacement plots derived from all records is

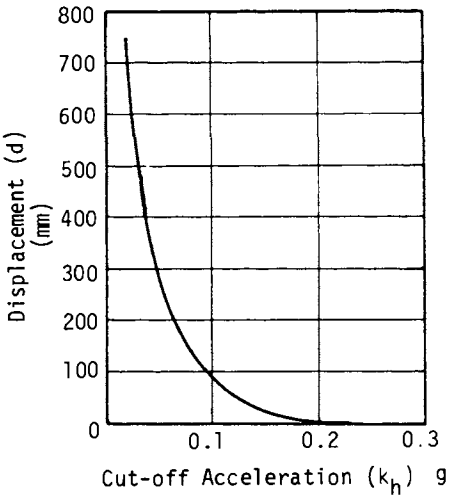

Figure 27. Maximum Wall Displacement Versus Limiting Acceleration for El Centro 1940 N-S Earthquake Record (after Richards and Elsm, 1979)

essentially the same (Richards and Elms, 1979). Franklin and Chang (1977) drew envelope curves for various groupings of acceleration records; their diagram is reproduced as Figure 28.

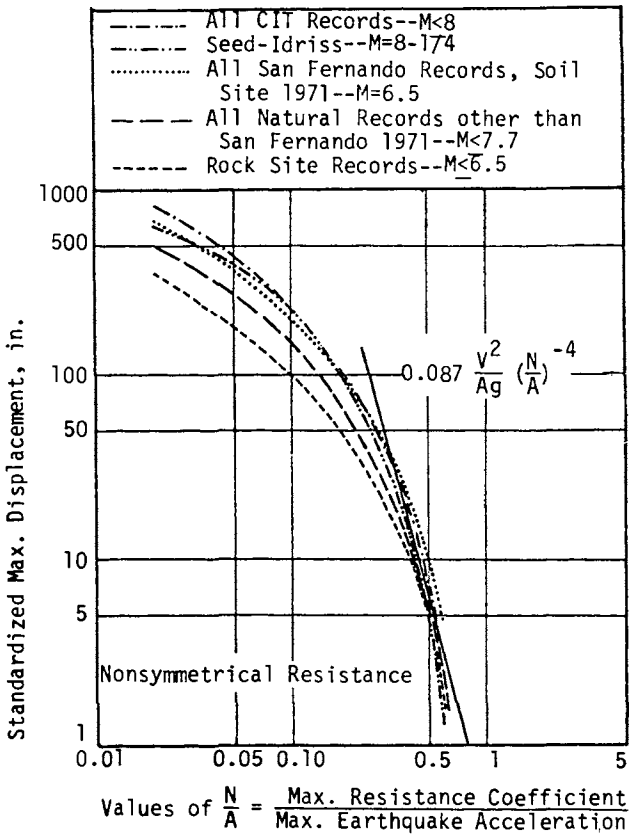

Figure 28. Upper Bound Envelope Curves of Permanent Displacements for all Natural and Synthetic Records Analysis by Franklin and Chang (after Richard and Elms, 1979).

Richards and Elms (1979) suggested a procedure for computing standardized maximum retaining wall displacements in the medium to low range that employs a suitable approximation of Franklin and Chang's curves. This is given by the expression

$$d = 0.087 \frac{V^2}{Ag} \left(\frac{N}{A}\right)^{-4} \text{ in.} \qquad (23)$$

in which d is the total relative displacement of a wall subjected to an earthquake record whose acceleration coefficient is A and maximum velocity is V in./sec. For a wall, N is of course equivalent to the limiting acceleration coefficient $(\alpha_h)_{cr}$ (Eq. 22a). This is drawn as a straight line in Figure 28. Richards and Elms (1979) state that this curve depends solely on the earthquake acceleration trace and not upon any retaining wall parameters or on the wall's manner of failure by sliding or tilting. The value of α_{cr} is dependent upon soil parameters. Also the wall displacement computed is in translation. Equation 22a suggests that α_{cr} considers limiting equilibrium in sliding. Therefore, rotation is not at all considered.

There are three objectives to this analysis:

1. The soil is assumed to be a rigid plastic material. The walls do undergo reasonable displacements before the limiting equilibrium conditions (active) develop and experience very large displacements before the passive conditions develop.

2. The natural period of the system is not considered.

3. Walls may undergo displacements by either sliding or tilting or both. This method does not apparently consider this difference in their physical behavior, although it is logical to conclude that displacements computed by this method is in sliding only.

Figure 2b shows that a wall moves away from the backfill during the first half cycle of ground motion. During the second half cycle, the wall tends to move towards the fill, but the resistance to this motion is far too great, and it is not physically possible for the wall to return to its original position. Thus, there is residual displacement of the wall away from the backfill. With every succeeding significant cycle of motion, the movement of the wall increases away from the backfill.

Now the movement of the wall may be either in translation, parallel to its original position, rotation about its heel, or a combined translation and rotation (which is usually the case). The soil stiffness on the two sides and the resistance of the base are nonlinear with displacement. Simple solutions for two cases--a wall undergoing sliding alone (Prakash and Nandkumaran, 1981a) and a wall undergoing rotation alone (Prakash et al., 1981b)--have been prepared at Roorkee and Rolla respectively. These are briefly described first, and their application to a typical case is demonstrated later.

Displacement Analysis in Translation

The force-displacement relationships, which are used in this analysis, are shown in Figure 29. The net force away from the fill is the difference of active earth pressure, c, and the base resistance, E (Fig. 29c). The net force towards the wall is the sum of the passive earth pressure, B, (Fig. 29a) and the base resistance, D (Fig. 29b). The resulting bilinear force-displacement relationship is shown in Figure 29d and is characterized by the following parameters: 1) Slope of force displacements on the active, k_1, and passive, k_2, sides respectively. 2) Yield displacement, z_y.

There is evidence to show that full active conditions develop if the wall displacement is 0.5 percent of its height away from the fill. Also, full passive resistance is mobilized if the wall translates 5 to 10% of its height towards the fill. However, to account for the steeper initial slope, a displacement of 0.25% of the wall height is taken for an active case and a displacement of 2.5% for a passive case. For the resistance of the base, it is assumed that a column of soil of height (B/2) tanϕ provides all of the resistance in a passive case (Fig. 30). In the figure, B is the width of the wall at its base (Prakash et al., 1981a).

The other parameters that are needed to define the system for displacement analysis are: 1) The mass in the system M, 2) Period of the wall-soil system, 3) Yield displacement, 4) Damping in the system, and 5) Parameters of ground motion.

The vibrating mass of the system consists of the mass of the wall and that of the soil vibrating with the wall. Nandkumaran (1973) conducted vibratory tests on translating walls and found that for the purpose of matching the computed frequency of the wall with the measured natural frequency the soil mass participating in the vibrations is 0.8 times the mass of soil on the Rankine failure wedge. Thus, by knowing the vibrating masses and the stiffness, as shown in Figure 29d, the natural period may be determined.

Yield displacements for a given wall can be determined by considering the force-displacement relationships in Figure 29.

There is no information on the damping of vibrating walls, therefore an arbitrary value has to be adopted.

The ground motion is considered to be a sinusoidal motion of definite magnitude and period.

The range of variables considered in this study are listed in Table 7.

Figure 31 shows a typical set of results in the form of slips per cycle versus the natural period of the wall in sec for the yield displacement z_y = 0.5 cm, ξ = 10%, and η = 2 and the ground motion of 300, 200 and 100 gals. Similar curves for all other ranges of variables listed in Table 7 have been as obtained (Prakash et al., 1981a). The ground motion is considered to be an equivalent motion of uniform peak acceleration of well defined cycles.

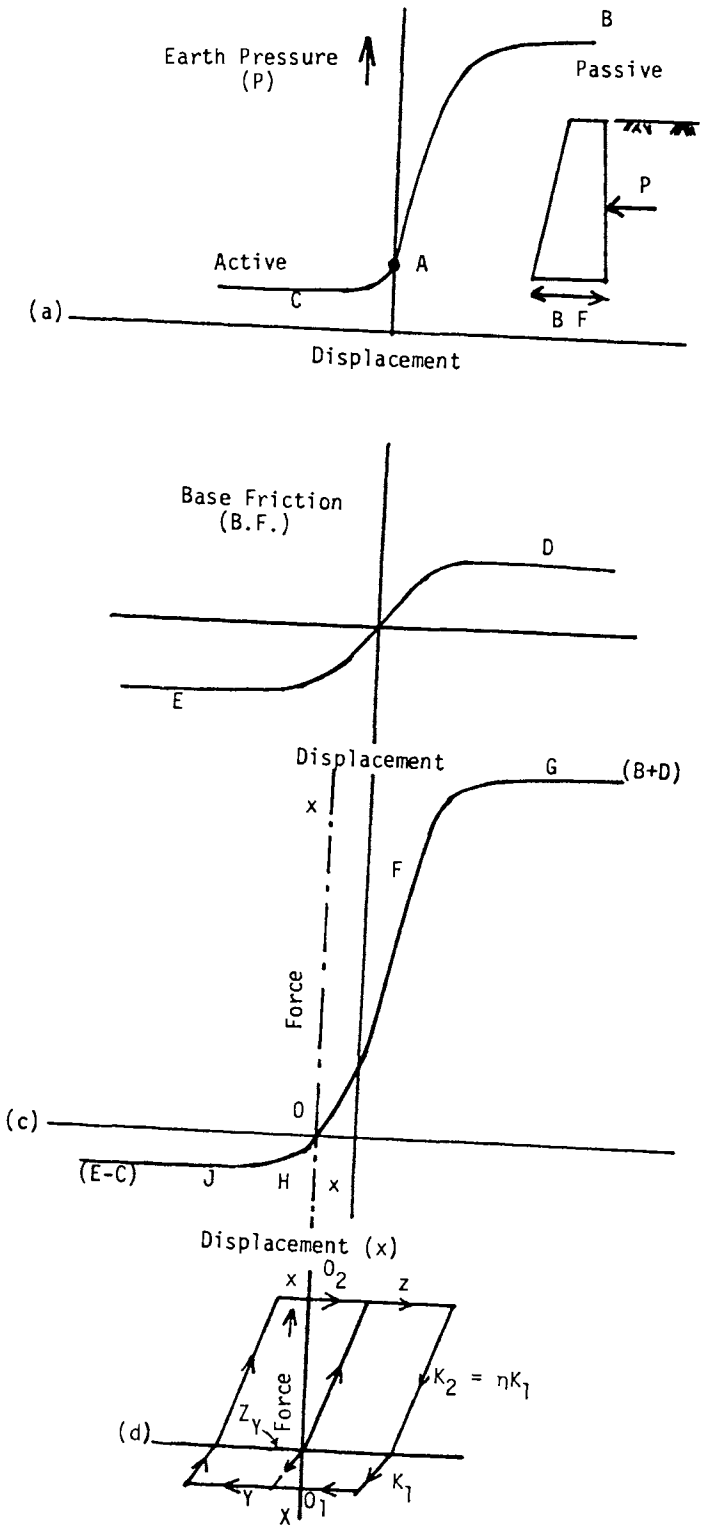

Figure 29.

a. Earth Pressure (P) Plot for Wall
b. Base-Friction (B.F.) vs Displacment
c. Resultant of 'P' and B.F. vs Displacement
d. Simplified bilinear Force-Displacement Diagram (after Nandakumaran, 1973, 1974)

Table 7*. Range of Variables

Ground acceleration amplitude (a) gals	100, 200, and 300
Period of ground motion (T) sec	0.5, 0.3, 0.2 and 0.1
Damping as fraction of critical damping (ζ) %	5, 10 and 15
Natural period T_n sec	1.0, 0.5, 0.3, and 0.2
Yield displacement (Z_y) cm	0.1, 0.2, 0.3, 0.5, and 1.0 cm
Ratio of stiffness (η)	2.0 and 3.0

*After Nandkumaran (1973)

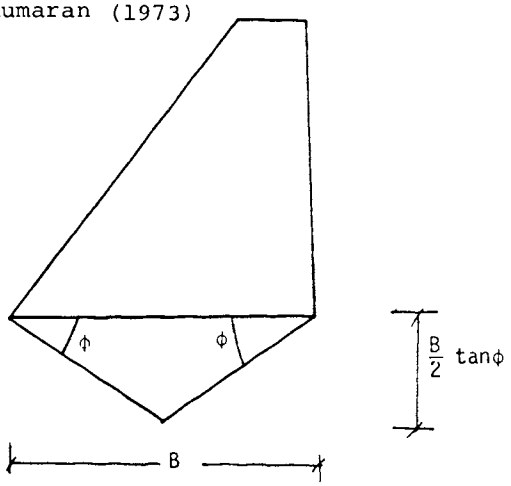

Figure 30. Proposed Method for Computation of Base Resistance (after Nandkumaran, 1973)

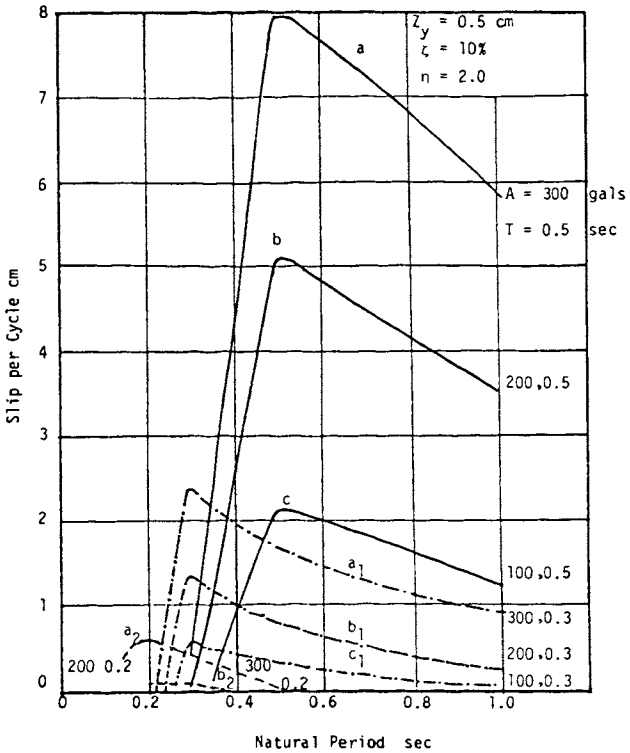

Figure 31. Natural Period vs Slip per Cycle (Z_y = 0.5cm)(after Nandakumaran, 1973, 1974)

The above analysis is better than the one proposed by Richards and Elms (1979) in that 1) definite procedure for determining the natural period of the soil-wall system in translation has been formulated, and 2) the physical behavior of the retaining wall is considered in developing the force-displacement relationships. The method, however, suffers from the fact that the tilting of the wall has not been considered. A simplified tilting analysis of the rigid retaining walls has been developed by Prakash et al., (1981b), which is now described.

Displacement Analysis in Rotation

Little information is available on the rotational displacement of retaining walls under dynamic loads. Analysis of Prakash et al., (1981b), for computing rotational displacement of rigid retaining walls is based upon the following assumptions:

1. Rocking vibrations are independent of sliding vibrations and the rocking stiffness is not affected by sliding of the wall.
2. The earthquake motion may be considered as an equivalent sinusoidal motion having constant peak acceleration.
3. Wall may be assumed to rotate about the heel.
4. Soil stiffness for rotational displacement of wall away from the backfill may be computed corresponding to average displacement for fully active motion.
5. Soil stiffness for rotational displacement of the wall towards the backfill may be computed corresponding to average displacment for development of fully passive conditions.
6. The stiffness values computed in 4 and 5 remain unchanged during phases of wall rotation towards and away from backfill respectively.
7. Soil participating in vibrations may be neglected.

The mathematical model based upon these simplifying assumptions is shown in Figure 32. Figure 33 shows the scheme for calculation of side resistance corresponding to active and passive conditions. If fully active conditions are assumed to develop at a displacement of 0.5% of height of wall, then K_A is given by Eq. 24 as per assumption 4

$$K_A = \frac{P_o - P_a}{\text{average displacement}} = \frac{\frac{k_o \gamma H^2}{2} - \frac{k_a \gamma H^2}{2}}{1/2\frac{(0.5\ H)}{100}} \quad (24)$$

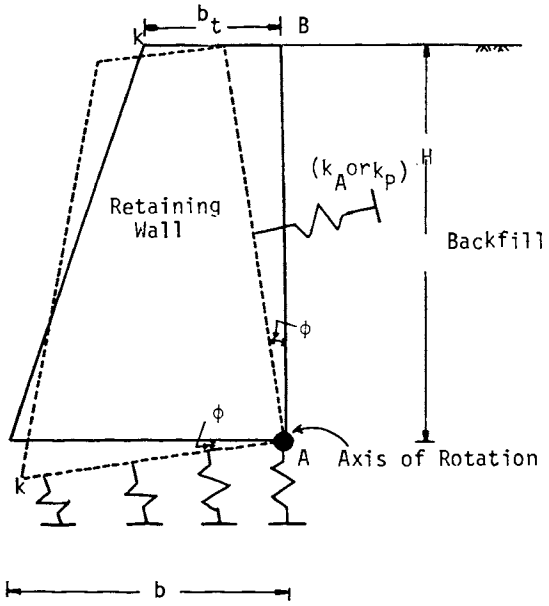

Figure 32. Mathematical Model for Rotations of Rigid Walls (after Prakash, Puri and Khandoker (1981)

in which K_A = stiffness of side spring under active conditions (FL^{-1}) and k_o and k_a are coefficients of at rest and active earth pressures respectively. Similarly if fully passive conditions are assumed to develop at 5% of wall displacement, K_p, may be computed according to Eq. 25.

$$K_P = \frac{P_p - P_o}{\text{average displacement}} = \frac{\frac{k_p \gamma H^2}{2} - \frac{k_o \gamma H^2}{2}}{1/2 \frac{(5H)}{100}} \quad (25)$$

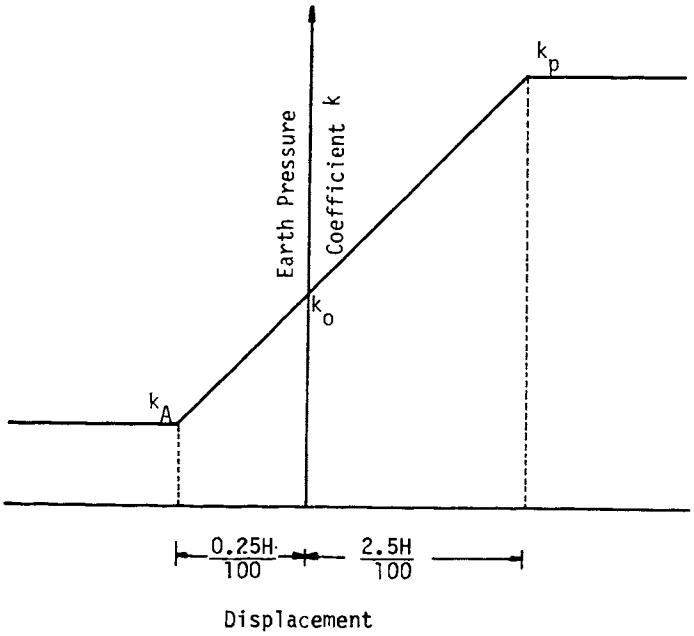

Figure 33. Scheme for Computation of Spring Stiffnesses

The rotational resistance of the base, M_R, may be represented by Eq. 26.

$$M_R = c_\phi \cdot I \cdot \phi \quad (26)$$

in which c_ϕ is coefficient of elastic nonuniform compression, I is moment of inertia of the base about an axes through the heel of the wall and perpendicular to the plane of vibrations and ϕ is angle of rotation.

The equations of motion for rotation of wall away and towards the backfill are

$$M_{mo} \ddot{\phi}_A + (c_\phi I - \frac{K_A H^2}{3})\phi_A = M(t) \quad (27a)$$

and

$$M_{mo} \ddot{\phi}_B + (c_\phi I + \frac{K_P H^2}{3}) = M(t) \quad (27b)$$

Since the stiffnesses K_A and K_P are different, the period of the wall for the two conditions, i.e., towards the backfill and away from the backfill would be different. This would result in different values of ϕ_A and ϕ_B for each half cycle of motion and net displacement of $(\phi_A - \phi_B)$ for one cycle of ground motion. The total displacement for any number of cycles may be computed as

$$\phi_T = N(\phi_A - \phi_B) \quad (28)$$

where N = number of equivalent uniform cycles of ground motion.

Based upon the above, a parametric study was made considering the following range of variables listed in Table 8.

It was observed that the contribution of rotational displacement may be significant for typical cases. The contribution of rotational displacement using the above approach was compared with the sliding displacement (Prakash et al., 1981) for the following case:

Height of wall	3.0 m
$\phi_{backfill}$	36°
Period of ground motion	0.3
α_h	0.25 g
c_ϕ	3 kg/cm^3

Total slip in 15 cycles due to sliding = 21.30c (Prakash and Nandakumaran, 1981). Total displacement at top of wall due to rotation = 14.7 cm.

This illustrates that the rotational displacement may not be negligible for this typical case and an attempt should be made to account for it.

The proposed analysis for rotational displacement is highly simplified. Nevertheless it shows explicitly that neglecting rational displacements may seriously underestimate the

Table 8.* Range of Variables

Height of wall m	3.0, 5, 7.5 and 10
$\phi_{backfill}$ (degrees)	30, 33 and 36
period of ground motion (sec)	0.3
damping values ζ %	0, 5, 10, 15
c_ϕ (base) kg/cm^3	3, 4, 5, 6 and 8
base width/height of wall	1/3

*After Prakash et al., 1981b.

total displacements in some cases. In actual practice it may be essential to account for combined effects of rocking and sliding that will affect the overall response of the system.

EARTH PRESSURES ON BASEMENT WALLS

The question of lateral pressures on basement walls is different than that on the free standing walls since basement walls do not undergo appreciable deformation under static or dynamic conditions. These are restrained at their top by floors and are acted upon by large vertical loads of the superstructure. This state is different than the active or passive conditions. Bishop (1958a,b) defined the coefficient of earth pressure at rest, k_o, as the ratio of the lateral to the vertical effective stress in a soil consolidated under the condition of no lateral deformation, the stresses being principal stresses with no shear stress applied to the planes on which these stresses act. Thus

$$k_o = \frac{\sigma'_h}{\sigma'_v} \qquad (29)$$

in which σ'_h = horizontal effective principal stress and σ'_v = vertical effective principal stress. Jaky (1948) has recommended values of k'_o in terms of soil parameters.

Tajimi (1973) presented a theoretical analysis of earth pressures on basement walls on the basis of the two-dimensional wave propagation theory. The walls were assumed to undergo periodic vibrations consisting of horizontal translation and rocking. The results are given for the distributions of earth pressure on the wall and the coefficients of soil reaction, which are expressed by real and imaginary components varying with frequency. Furthermore, the theoretical predictions were examined by field experiments of moderate scale.

Niwa (1971) measured oscillating earth pressures acting on the back of a gravity type test retaining wall made of concrete 3m high, 0.6m wide at the top, 1.5m wide at the bottom and 5m in length. It was placed on the bottom of a trench which was excavated in loam* soil up to 3m depth. The trench had a slope on the side facing the back of the test wall, which was backfilled by sand. To excite the horizontal translation of the wall, the sinusoidal ground motion was generated by a large rotating mass-shaking machine which was embedded in the ground at a distance of 12m from the test wall. In addition, a small vibration exciter was mounted on the top of the wall in order to produce rocking. The displacements were measured at the top and bottom.

Figure 34. shows typical results of earth pressures with varying frequencies observed during the ground motion test. In this test, the amplitude of displacement at the bottom was of the order of 0.3mm at the frequency about 6Hz. The measured results were compared with the theory of horizontal translation, because the rocking mode was observed very little. From comparison, a common feature was recognized that the magnitude of pressure increases with depth.

For the case of rocking, a similar comparison was examined. The experimental results of earth pressure are shown in Figure 35. Again a comparison with analytical results appear to agree as a trend. In the quantitative comparison, the theoretical and observed earth pressures could be roughly coincided with each other, if the shear modulus of sand is assumed as G = 100 kg/cm^2. In this test, the amplitude of displacement at the top was of order of 0.44mm at frequency about 8.3Hz. Tajimi (1973) recommends that it would be useful to develop an equivalent mass-spring-dashpot system representing embedded structures. Ikuta et al., (1979) measured earth pressure and water pressure on the perimeter basement walls of a building during the Off Miyagi Prefecture Earthquake (Magnitude 7.1) on 12th June 1978. The building was located about 380km away from the epicenter. The seismic intensity of the earthquake in Yokohama City was judged to be "IV" according to the seismic intensity scales defined by the Japan meteorological Agency (JMA). Maximum acceleration at the 2nd basement of this building was about 0.125g. The building was a high-rise office building with two basement floors and 27 stories above the ground. The foundation consisted of cast-in-place piles and basement walls which also served as piling wall. The soil profile of the building site comprised a thick alluvial deposit of soft silt which reached the hard support layer of the diluvial deposit at a depth of 22 to 28m. The basement structure and basement walls were rigidly connected with shear connectors. The record was obtained from 7 points out of 26 points of earth pressure gauges and 3 points out of 7 points of water pressure gauges.

The maximum amplitude of pressure 'Δp' corresponding to p, during the earthquake and the ratio between the two values were shown (Table 8). The maximum amplitudes of pressure Δp were within the range of 2.74 to 6.37 kN/m^2 and tended to become larger when closer to the ground surface. The ratios $\Delta p/p$ were within the range of 0.011 to 0.374.

*probably sandy soil (author)

Table 8. Quantities of Fluctuations of Earth Pressure Due to Earthquake (after Ikuta et al., 1979)

	No.	Depth (m)	p (kN/m^2)	Δp (kN/m^2)	$\Delta p/p \times 100\%$
S Side Earth Pressure	1	8.3	72.13	5.68	7.88
	2	15.8	176.20	3.53	2.00
	3	18.8	225.89	3.72	1.65
	4	20.3	246.08	2.74	1.11
E Side Earth Pressure	5	4.2	17.05	6.37	37.36
	6	18.2	104.96	4.21	4.01

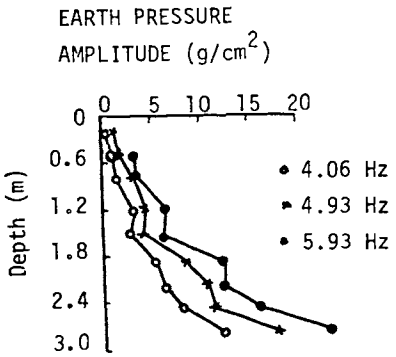

Figure 34. Experimental Distribution of Earth Pressure Amplitude (sway) after Niwa (1971)

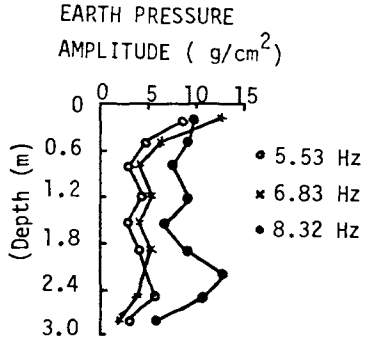

Figure 35. Experimental Distribution of Earth Pressure Amplitude (rocking)

On the basis of these observations and the attendant analysis, it was concluded that the flucuations of earth pressure during the earthquake became greater when closer to the ground surface. Even during the earthquake under consideration here, earth pressure fluctuated nearly 40% over normal time. The earth pressure during the earthquake closely resembled those wich appeared on the ground displacement record. Taylor and Indrawan (1981) have analyzed this data further in their paper to this conference.

Hall (1978) suggested a technique (Figure 36) for adjusting the results of the Mononobe-Okabe equations to account for the initial at-rest earth pressure. The procedure is to compute the dynamic earth pressure coefficient for both the active and passive conditions and plot these as a function of the corresponding static earth pressure coefficients. The dynamic earth pressure coefficient corresponding to the at-rest pressure may then be interpolated linearly between the two limits.

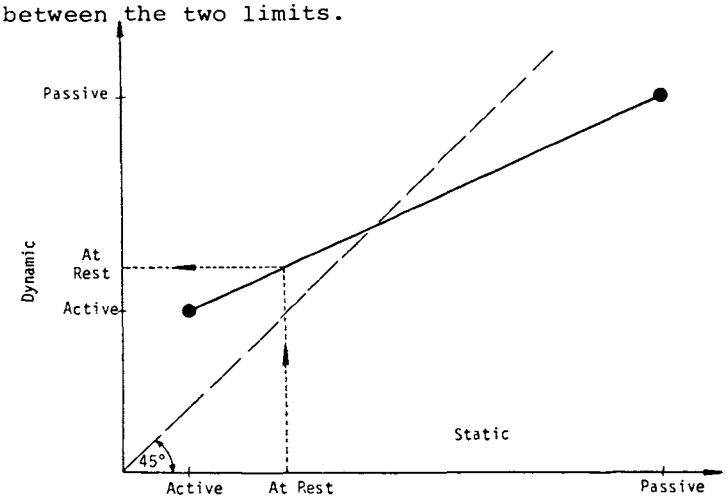

Figure 36. Interpolation of Mononobe-Okabe Formulas for At-Rest Pressure Conditions (after Hall, 1978)

It is of interest to note that the Mononobe-Okabe theory predicts that for the active static condition, the wall pressures will increase, whereas, for the passive static condition, the wall pressures will decrease. This is consistent with the assumption that the active and passive earth pressures represent upper and lower bounds.

However, Prakash (1981) recommends that since static "at rest" earth pressures are higher than the active earth pressures, it is likely that earth pressures during earthquakes on basement walls (corresponding to at rest conditions in static case) may also be higher than the total (static & dynamic) earth pressures in the active condition. It is tentatively recommended that percentage increases in earth pressure over the static at rest pressures be assumed equal to the percentage increases in active earth pressures under dynamic conditions. No rational explanation can be offered for this recommendation at present but the pressures so computed are likely to be considerably higher than those based upon the recommendation of Hall (1978).

It will be seen that the question of dynamic increases in at rest earth pressure has been studied to a very small extent. The resulting increases in earth pressure obtained from different recommendations and test data summarized here will be quite different and the scatter may also be large. Therefore, there is a need to study this question in detail both analytically and experimentally.

Table 9. Building Code Requirements for Lateral Pressures During Earthquakes

Country	Year	No Indication of Special Requirement	Method of Computing Lateral Pressure for Earthquake Loading
Canada*	1953	x	
France	1967		Horizontal and vertical seismic coefficients are 0.1α, where α is the intensity coefficient.
Greece*	1958		Mononobe-Okabe formula with k_h varying from 0.08 to 0.32 depending on seismic zone and foundation conditions.
India	1975		Mononobe-Okabe formula using horizontal and vertical seismic coefficient from consideration of foundation conditions and inertia force of the wall. Point of application of dynamic increment at 1/2H above base. Also, the resultant of all the forces shall fall within the middle 3/4 of the base width.
Italy*	1937	x	
Japan	1973		Mononobe-Okabe analysis with seismic coefficient as seismic coefficient = regional seismic coefficient x factor for subsoil condition x importance factor Also, the resultant vector of all the forces shall not fall beyond 1/4 of the base length from the center of the base. However, this proportion may be increased up to 1/3 for a strong foundation.
Mexico	1975		Mononobe method for computation of earth pressure.
New Zealand*	1955	x	
Philippines*	1959	x	
Portugal*	1958		Design must consider seismic forces, for waterfront structures dynamic pressures of water on structures must be considered
Turkey	1975		For design of retaining walls angle of shearing strength to be reduced by 6° in 1st and 2nd degree earthquake zones and 3° in 3rd and 4th degree earthquake zones.
Venezuela*	1959	x	
U.S.A.			
1 TVA*	1939		Mononobe-Okabe analysis with $k_h = 0.18$.
2 ATC	1978	x	
USSR	1969	x	

*After Seed and Whitman (1970)

CODAL PROVISIONS

Codes for design of structures against earthquakes have been issued and updated from time to time. In several of these codes, provisions have been made to account for changes in the earth pressure due to seismic action. However, no mention is made of permissible displacements. Table 9 lists building code requirements for lateral pressures during earthquakes of several countries.

FURTHER WORK

In order to study the dynamic lateral stresses exerted against retaining structures during earthquakes, Sherif et al., (1980) have designed and constructed a shaking table 8 feet long, 6 feet wide and 4 feet high, and is excited either discretely or randomly by a closed loop MTS hydraulic system.

A model retaining wall has been constructed to sit within the shaking table so that it can undergo several kinds of movement. Using this system, the neutral, active or passive stresses exerted against the wall as a function of wall movement can be investigated.

The model wall which is 5' 10-3/8" wide, 3' 5" high and 11-1/2" thick is basically composed of two parts, the center wall and the main frame which includes side walls. The center wall itself is 3' 4" wide, 3' 5" high and 5" thick and it is built into the main body of the model wall. In order to reduce the boundary effects, only the center wall is instrumented by load cells, stress and pore water pressure measuring transducers. Two independently controlled wall driving mechanisms, one near the top and the other near the bottom of the wall, provide various kinds of lateral wall movements. Each wall driving systen is powered by a variable speed motor. The deformation of the wall is measured by two LVDT's attached to the center wall. The data generated by the transducers, LVDT's, load cells and accelerometers are monitored by a high capacity data acquisition system.

A detailed investigation of the question of static and dynamic earth pressures and displacement analyses of the walls has been planned at several other institutions including M.I.T., University of Missouri-Rolla, Missouri and University of Roorkee, Roorkee, India, and in France and New Zealand.

DISCUSSION AND CONCLUSIONS

The problems of earth pressure variation due to earthquake motion, point of application of the dynamic increment, and displacement of the wall have been highlighted.

There is a general agreement that the dynamic increment in active earth pressure be determined from Mononobe-Okabe method. The seismic coefficient for this determination has been correlated with the peak ground velocity of a site.

The center of dynamic earth pressure increment has been shown to act at 0.55H and 0.45H above the base of flexible and rigid walls respectively.

Three methods of computation of displacements of rigid retaining walls have been included; 1) Richards and Elms (1979) method based on Newmark's (1965) concept of sliding surfaces, 2) Prakash et al., (1981a) method for computing translational displacements and 3) Prakash et al., (1981a) method for computing rotational displacements.

Limitations and advantages of the three methods have been discussed and the need for development of a versatile model to account for translation and rotation simultaneously has been highlighted.

The question of passive earth pressures on abutments and earth pressures on basement walls have also been discussed.

There are several problems in earth pressures which have not been addressed at all or adequately in this report. These are

1. Effects of saturation and submergence on the earth pressures and displacements and attendant hydro-dynamic pressures.
2. Solutions for uniform and sloping backfills for c-ϕ soils.
3. Solutions for sheet-pile cantilever walls and anchored bulkheads.
4. Further work is needed on dynamic passive pressures and pressures on basement walls.
5. Development of a more general model to compute displacements of walls both in sliding and rotation and possible sinking also.
6. Correlation of experimental work with analytical solutions.
7. To define: what constitutes a permissible displacement of a wall?

There is a great need to observe the behavior of retaining walls more extensively with attendant soil property determination after an earthquake to develop rational approach for prediction of displacements at design stage consistant with observed mode of failure. Carefully planned full scale tests on test walls, though expensive, will provide useful information in this direction.

ACKNOWLEDGEMENTS

Vijay K. Puri commented on the draft of the paper and offered several critical but useful suggestions. Mrs. Aleen Donovan of EERC--University of California searched some useful literature for preparation of this report. Padmaker Srivastava drafted all the figures and Margot Lewis typed it with great care. All this assistance is acknowledged.

REFERENCES

Aggour, M.S. and C.B. Brown (1973), "Retaining Wall in Seismic Areas", Proc., 5th World Conference on Earthquake Engineering, Rome.

Aliev, H., H. Mamedov and T. Radgabova (1973), "Investigation of the Seismic Pressure of Soils on the Retaining Walls and Interdependence Between Foundation Soils and Constructions", Proc., Symposium on Behaviour of Earth and Earth Structures, Roorkee, March, Vol. 1.

Arya, A.S. and Y.P. Gupta (1966), "Dynamic Earth Pressures on Retaining Walls Due to Ground Excitations", Bull., Indian Society of Earthquake Technology, Roorkee, Vol. III, No. 2.

Basavanna, B.M. (1970), "Dynamic Earth Pressure Distribution behind Retaining Walls", Proc., 4th Symposium on Earthquake Engineering, University of Roorkee, Roorkee.

Basudhar, P.K. and M.R. Madhav (1980), "Simplified Passive Earth Pressure Analysis", J. Geotechnical Engineering Division, ASCE, Vol. 106, No. GT4, April, pp. 470-479.

Bishop, A.W. (1958a), "Test Requirements for Measuring the Coefficient of Earth Pressure at Rest", Proc., Brussels Conference on Earth Pressure Problems, Vol. 1, pp. 2-14.

Bishop, A.W. (1958b), "Discussion", Proc., Brussels Conference on Earth Pressure Problems, Vol. 3, pp. 36-39.

Clough, G.W. and R.F. Fragaszy (1977), "A Study of Earth Loadings on Flood Way Retaining Structures in the 1971 San Fernando Valley Earthquake, Proc., 6th World Conference on Earthquake Engineering, New Delhi, India, pp. 2455-2460.

Coulomb, C.A. (1 73), "Essai sur une application des regles des maximis et minimis a quelque problems de statique relalifs a 1' architecture'. Mem. acad. roy. pres. diverssavants, Vol. 7, Paris.

Evans, G.L. (1971), "The Behavior of Bridges Under Earthquake", Proc., New Zealand Road Engg. Symposium, Victoria University of Wellington, Wellington, New Zealand, Vol. 2, pp. 664-684.

Franklin, A.G. and F.K. Chang (1977), "Earthquake Resistance of Earth and Rock-Fill Dams", Report 5: Permanent Displacements of Earth Embankments by Newmark Sliding Block Analysis", Misc. Paper S-71-17, Soils and Pavements Laboratory, U.S. Army Engineer Waterways Experiment Station, Vicksburg, MS, November.

Hall, J.R. Jr. (1978), "Comments on Lateral Forces--Active and Passive", Proc., ASCE Specialty Conference on Earthquake Engineering and Soil Dynamics, Pasadena, CA, June, pp. 1436-1441.

Ichihara, M., S. Umebayashi and H. Matsuzawa (1977), "Passive Earth Pressure and Deformation of Overconsolidated Soft Clay", Proc., International Symposium on Soft Clay, Bangkok, Thailand, July.

Ikuta, Y., M. Maruoka, T. Mitoma and M. Naganou (1979), "Record of Lateral Pressure Taken During Earthquake", Soils and Foundations, Tokyo, Vol. 19, No. 4, December, pp. 85-89.

Indian Standard Recommendations for Earthquake Resistant Design of Structures, IS: 1893-1975 (Third Revision).

Ishii, Y., H. Arai and H. Tsuchida (1960), "Lateral Earth Pressure in an Earthquake", Proc., 2nd World Conference in Earthquake Engineering, Tokyo, Vol. 1, p. 211.

Jacobsen, L.S. (1951), "Kentucky Project Report No. 13", TVA Series 1951, Appendix D.

Jakovlev, P.I. (1977), "Coefficients of Active and Passive Earth Pressure on Retaining Walls Under Seismic Conditions", Proc. VI, World Conference on Earthquake Engineering, Vol. II, pp. 2356-2362, January, New Delhi.

Jaky, J. (1944), "The Coefficient of Earth Pressure at Rest", Journal of the Society of Hungarian Architects and Engineers, Budapest, Hungary, pp. 355-358.

Jaky, J. (1948), "Pressure in Silos", Proc., 2nd International Conference on Soil Mechanics and Foundation Engineering, Vol. 1, pp. 103-107.

Kapila, I.P. (1962), "Earthquake Resistant Design of Retaining Walls", 2nd Symposium on Earthquake Engineering, University of Roorkee, Roorkee, pp. 97-108.

Krishna, J., S. Prakash and P. Nandakumaran (1974), "Dynamic Earth Pressure Distribution Behind Flexible Retaining Walls", Journal, Indian Geotechnical Society, Vol. 4, No. 3, July, pp. 207-224.

Madhav, M.R. and N.S.K. Rao (1969), "Earth Pressures Under Seismic Conditions", Soils and Foundations, Japan, Vol. IX, No. 4.

Matsuo, H. (1941), "Experimental Study on The Distribution of Earth Pressure Acting on a Vertical Wall During Earthquakes", Journal, Japanese Society of Civil Engineering, Vol. 27, No. 2.

Matsuo, H. and S. Ohara (1960), "Lateral Earth Pressure and Stability of Quay Walls During Earthquakes", Proc., 2nd World Conference on Earthquake Engineering, Tokyo, Vol. 1, pp. 165-183.

Mononobe, H. (1929), "Earthquake Proof Construction of Masonry Dams", Proc., World Engineering Congress, Vol. 9, p. 275.

Mononobe, N. and H. Matsuo (1929), "On the Determination of Earth Pressures During Earthquakes", Proc., World Engineering Conference, Vol. 9, p. 176.

Murphy, V.A. (1960), "The Effect of Ground Characteristics on the Aseismic Design of Structures", Proc., 2nd World Conference on Earthquake Engineering, Tokyo, Japan.

Nandakumaran, P. (1973), "Behaviour of Retaining Walls Under Dynamic Loads", Ph.D. Thesis, Roorkee University, Roorkee, India.

Nandakumaran, P. (1974), "Behavior of Retaining Walls During Earthquakes", Chapter 17 in "Earthquake Engineering", Jai Krishna 60th Anniversary Volume, Sarita Prakashan, Meerut, U.P.

Nandakumaran, P. and V.H. Joshi (1973), "Static and Dynamic Active Earth Pressures Behind Retaining Walls", Bull. Indian Society of Earthquake Technology, Sept., Vol. 10, No. 3.

Narain, J., S. Saran and P. Nandakumaran (1969), "A Model Study of Passive Pressures in Sand", Journal, Soil Mechanics and Foundation Div., ASCE, Vol. 95, No. SM4, July.

Nazarian, H.N. and A.H. Hadjian (1979), "Earthquake-Induced Lateral Soil Pressures on Structures", Journal, Geotechnical Engineering, ASCE, Vol. 105, No. GT9, pp. 1049-1066, September.

Newmark, N.M. (1965), "Effect of Earthquakes on Dams and Embankments", Geotechnique, Vol. 15, No. 2, pp. 139-160.

Niwa, S. (1960), "An Experimental Study of Oscillating Earth Pressures Acting on a Quay Wall", Proc., 2nd World Conference on Earthquake Engineering, Tokyo, Japan.

Niwa, S. (1971), "An Experimental Study of Oscillating Earth Pressure Acting on a Gravity Wall", Report of Ship Research Institute, Vol. 8, No. 5, September (in Japanese).

Okabe, S. (1924), "General Theory on Earth Pressure and Seismic Stability of Retaining Walls and Dams", Journal, Japan Society of Civil Engineers, Vol. 6.

Okabe, S. (1926), "General Theory of Earth Pressures", Journal, Japanese Society of Civil Engineers, Tokyo, Japan, Vol. 12, No. 1.

Prakash, S. (1981), Soil Dynamics, McGraw Hill Book Co., New York, NY.

Prakash, S. and B.M. Basavanna (1969), "Earth Pressure Distribution Behind Retaining Walls During an Earthquake", Proc., 4th World Conference in Earthquake Engineering, Santiago, Chile.

Prakash, S. and P. Nandkumaran (1969), "Earth Pressure Distribution on Flexible Walls with Rigid Foundations During Earthquakes", (unpublished) Earthquake Engineering Studies, University of Roorkee, Roorkee, India.

Prakash, S. and P. Nandakumaran (1973), "Dynamic Earth Pressure Distribution on Rigid Walls", Proc., Symposium on Earth and Earth Structures Subjected to Earthquakes and Other Dynamic Loads, Roorkee, March, Vol. 1, pp. 11-16.

Prakash, S. and P. Nandakumaran (1979), "Earth Pressures During Earthquakes", Proc., 2nd U.S. National Symposium on Earthquake Engineering, Stanford, pp. 613-622, August.

Prakash, S., P. Nandakumaran and J. Krishna (1981), "Displacement Analysis of Rigid Retaining Walls During Earthquakes", Unpublished Report, Univ. of MO-Rolla, Rolla, MO.

Prakash, S., V.K. Puri and J.U. Khandoker (1981) "Rocking Displacements of Rigid Retaining Walls During Earthquakes", Companion paper to Conference on Recent Advances in Geotechnical Earthquake Engineering and Soil Dynamics, Vol. 3, St. Louis, MO, April-May.

Prakash, S., G. Ranjan and S. Saran (1979), "Analysis and Design of Foundations and Retaining Structures", Sarita Prakashan, Meerut, India.

Prakash, S. and S. Saran (1966), "Static and Dynamic Earth Pressures Behind Retaining Walls", Proc., 3rd Symposium on Earthquake Engineering, University of Roorkee, Roorkee, India, Vol. 1, pp. 277-288.

Rankine, W.J.M. (1857), "On the Stability of Loose Earth", Phi. Trans. Royal Soc., London.

Richards, R. Jr. and D.G. Elms (1979), "Seismic Behavior of Gravity Retaining Walls", Journal, Geotech. Eng. Div., ASCE, Vol. 105, No. GT4, April, pp. 449-464.

Sabzaveri, A. and A. Grahramani (1974), Dynamic Passive Earth Pressure Problem", Journal, Geotech. Eng. Div., ASCE, Vol. 100, No. GT1, pp. 15-30.

Sano, R. (1916), "Theory of Aseismic Design of Buildings", Report of Imperial Earthquake Investigation Committee, Vol. 83, A.

Saran, S. and S. Prakash (1968), "Dimensionless Parameters for Statick and Dynamic Earth Pressures Behind Retaining Walls", Journal, Indian National Society of Soil Mechanics and Foundation Engineering, July, pp. 295-310.

Scott, R.F. (1973), "Earthquake Induced Earth Pressures on Retaining Walls", Proc., 5th World Conference on Earthquake Engineering, Rome, Vol. 2, p. 1611.

Seed, H.B. and R.V. Whitman (1970), "Design of Earth Retaining Structures for Dynamic Loads", ASCE Specialty Conference on Lateral Stresses in the Ground and Design of Earth Retaining Structures, pp. 103-147, Ithaca, NY.

Sherif, M.A., I. Ishibashi and C.D. Lee (1980), "Dynamic Lateral Earth Pressures Against Retaining Structures", University of Washington Soil Engineering Research Report, No. 21, November.

Shields, D.H. and A.Z. Tolunay (1955), "Passive Pressure Coefficients by the Method of Slices", Journal, Soil Mechanics and Foundations, ASCE, Vol. 99, No. SM12, December, pp. 1043-1053.

Sim, L.C. and J.B. Berrill (1979), "Shaking Table Tests on a Model Retaining Wall", paper presented to the South Pacific Regional Conference on Earthquake Engineering, Wellington, New Zealand, May.

Sokolovski, V.V. (1960), Statics of Soil Media, Butterworths, London.

Tajimi, H. (1973), "Dynamic Earth Pressures on Basement Wall", Proc., 5th World Conference on Earthquake Engineering, Rome, Vol. 2, pp. 1560-1569.

Taylor, P.W. (1981), "A Simple Method of Estimating Seismic Pressures from Cohesive Soils Against Basement Walls", Proc., International Conference on Recent Advances in Geotechnical Engineering and Soil Dynamics, St. Louis, MO, April-May, Vol. 1.

Terzaghi, K. (1936), "A Fundamental Fallacy in Earth Pressure Computations", Contributions to Soil Mechanics 1925 to 1940, Boston Society of Civil Engineers.

Terzaghi, K. (1943), Theoretical Soil Mechanics, John Wiley and Sons, New York, NY.

Terzaghi, K. and R.B. Peck (1967), Soil Mechanics in Engineering Practice, 2nd Edition, John Wiley and Sons, New York, NY.

Woods, J.H. (1973), "Earthquake-Induced Soil Pressures on Structures", Report EERL, 73-05, Earthquake Engineering Research Laboratory, California Institute of Technology, Pasadena, CA.